https://doi.org/10.5194/egusphere-2026-3269
Preprint. Discussion started: 19 June 2026

Can bias correction methods improve the statistical characterization of extreme rainfall compound events in climate simulations?

Grégoire Jacquemin[1,2,a], Mathieu Vrac[2,3,b], Xavier Freulon[1,c], and Denis Allard[4,d]

[1]Mines Paris, PSL University, Centre for geosciences and geoengineering, 77300 Fontainebleau, France
[2]Laboratoire des Sciences du Climat et l'Environnement (LSCE), CEA, CNRS, UVSQ, Université Paris-Saclay, UMR8212, 91191 Gif-sur-Yvette, France
[3]Institut Pierre Simon Laplace (IPSL), FR636, Paris, France
[4]Biostatistiques et Processus Spatiaux (BioSP), INRAE, Avignon, 84914, France
[a]*gregoire.jacquemin@minesparis.psl.eu*
[b]*mathieu.vrac@lsce.ipsl.fr*
[c]*xavier.freulon@minesparis.psl.eu*
[d]*denis.allard@inrae.fr*

Abstract. Compound events (CEs), commonly defined as the "combination of multiple drivers and/or hazards that contributes to societal or environmental risk", often result in amplified impacts compared to individual hazards. To understand their evolution in terms of frequency under climate change, the outputs of climate simulations are used. Climate simulations are often statistically biased which can affect the representation of CEs. Hence, this study examines to what extends bias correction methods, including multivariate ones, improve the statistical characterization of CEs. It also aims at determining whether their evolution under climate change can be preserved by these methods. Two extreme rainfall events triggered by accumulated precipitation have been selected and analyzed either with a multivariate generalized Pareto modeling or a copula-based modeling. Two multivariate bias correction methods (dOTC and R^2D^2) and one univariate bias correction method (CDF-t) are applied to bias correct simulations from 10 global climate models. Bias corrected and raw data are compared in terms of return periods and in terms of extremal dependence structure. The results show that bias correction methods improve the representation of the two studied CEs and that the sign of their evolution is preserved in most cases.

Keywords Bivariate Extremes, CDF-t, dOTC, R^2D^2, Asymptotic Dependence, Return Periods, Climate Change, Extremal Index, Antecedent Precipitation Index

1 Introduction

In early June 2016, the Seine and the Loire rivers flooded simultaneously, causing more than one billion euros in damages and three fatalities across France (van Oldenborgh et al., 2016). Another catastrophic event occurred on 14th July 2021 in Germany and Belgium: extremely intense precipitation triggered the flooding of the Ahr catchment, resulting in more than

https://doi.org/10.5194/egusphere-2026-3269
Preprint. Discussion started: 19 June 2026

30 billion euros of damages and more than 200 deaths. High soil moisture levels previous to the precipitation are understood to have amplified surface runoff and thereby the severity of the inundation (Mohr et al., 2023). Both events share a defining characteristic: they arose from the combination of two individual extreme events, the flooding of the Seine and the flooding of the Loire for the former and the extreme precipitation and the high soil moisture level for the latter.

Such events are called compound events (CEs), which Zscheischler et al. (2020) define as the "combination of multiple drivers and/or hazards that contributes to societal or environmental risk". The two previously mentioned events are example of CEs. Such combinations can amplify the impact of individual hazards, often leading to a more severe impact. Although the understanding, analysis and projection of CEs remain in their early stages, their study is primordial in a climate change context to anticipate the evolution of existing risks and to prevent new risks to arise (Brett et al., 2025). Accurately capturing these events requires a comprehensive and sophisticated statistical modeling of the dependence structure between the variables, in particular in tails of the distribution (Bevacqua et al., 2017; Yang et al., 2023; Xu et al., 2023; Jacquemin et al., 2026).

Climate change is expected to modify the distribution of individual climate variables, such as temperature and precipitation, but may also influence the interactions between these variables, their spatial interactions (François and Vrac, 2023) and the outputs of process models driven by these variables (Allard et al., 2025). Concerns have also arisen about the possibility that compound events may become more frequent in the future under climate change. The changes in distribution and dependence may lead to complex evolutions in the frequency of compound events under future climate conditions (Zscheischler et al., 2018; Ridder et al., 2022; Heinrich et al., 2023). Recent developments in the study of the evolution of climate-related disasters have highlighted the strong correlation between the frequency and magnitude of certain extreme events and the global warming level (temperature extremes in Seneviratne et al. (2016) and precipitation extremes in Li et al. (2019) for example). Projection of CEs-related disasters in a future climate has thus become a major research question (Kharin et al., 2018).

Projecting future changes in the frequency of extreme events is usually based on outputs from climate simulations. However, climate simulations are often statistically biased (Raäisaänen, 2007; Christensen et al., 2008), meaning that the statistical properties of simulated climate variables (mean, variance, extreme quantiles and, more generally, the overall distribution) can differ from the properties of reference variables (e.g., reanalyses, weather station measurements). To address these discrepancies, a well-formed body of methods for Bias Correction (BC) has been developed. Statistical differences between observations and simulations are learned over a past "calibration" period, and simulations are then corrected over a "projection" period, usually in the future. Over the past decades, several univariate BC methods have been proposed. These include the Delta change method (correction of the mean, Gleick, 1986; Hay et al., 2000), the linear regression (Maraun et al., 2010), or the quantile mapping and its different variants, introduced in Panofsky and Brier (1958) and later applied by Haddad and Rosenfeld (1997) and Déqué (2007) for example. Finally, the CDF-t method proposed by Michelangeli et al. (2009) has the advantage to account for non-stationarity between the calibration and the projection (Vrac et al., 2012). However, univariate BC methods are designed to correct variables separately from each other, which means that the dependence structure between the variables is not corrected or even modified (Vrac, 2018). Hence, if the climate model dependence is biased with respect to the reference one, it will still be biased after a quantile-based univariate BC. In such a case, to project the evolution of compound events, multivariate BC methods are required to ensure that both the variables and the dependence structure between them are corrected.

https://doi.org/10.5194/egusphere-2026-3269
Preprint. Discussion started: 19 June 2026

Among the existing multivariate BC methods, the matrix recorrelation method (MRec) was introduced by Bárdossy and Pegram (2012) and used in Pegram and Bárdossy (2013) and El Hachem et al. (2025). This method first transforms the marginals into Gaussian distributions, then reconstruct the dependence structure of the reference with the Pearson cross-correlation matrices. Hence, this method is not adapted for non-Gaussian climate variables (François et al., 2020) like precipitation, the main variable used in this study. Another method, the Multivariate Bias Correction with N-dimensional probability density function transform (MBCn), has been introduced by Cannon (2018) and used in Adeyeri et al. (2020); Dieng et al. (2022); Meng et al. (2022); Olschewski et al. (2024). A random orthogonal matrix is iteratively applied to the matrix of the bias-corrected marginals, until the multivariate distribution matches the one of the reference. However, this method is potentially instable and it brings undesired stochasticity in the correction (François et al., 2020). Some studies have developed multivariate BC methods attempting to adjust the temporal correlation of the variables on multiple timescales in addition to correcting the inter-variables dependence (Mehrotra and Sharma, 2015, 2016, 2019). Statistics of interest are corrected towards those of daily observations and then aggregated up to yearly timescales. This temporal feature is not of interest in this study, as the CEs considered here are seasonal, and only the daily timescale is relevant. The dynamical Optimal Transport Correction (dOTC, Robin et al., 2019) relies on optimal transport theory to bias correct multivariate dimensions. The method is able to correct the dependence structure and to account for temporal non-stationarities, both for the margins and the dependence structure. Finally, the Rank Resampling for Distributions and Dependences (R^2D^2, Vrac, 2018) method first corrects the marginals with a univariate BC method, then reconstruct the dependence structure based on the rank evolution of a pivot variable. R^2D^2 is based on the assumption of stability in time of the dependence structure and also provides some stochasticity to investigate climate uncertainties.

Multivariate BC methods have already been employed to correct compound events. For example, the performance of two multivariate BC methods, MBCn and one of its variants MBCr (Cannon, 2018), is evaluated in Meng et al. (2022) on the representation of compound hot and dry events within 20 CMIP6 simulations. Their study highlights a better representation of the dependence between temperature and precipitation with the use of multivariate BC, as well as a number of CEs closer to that of observations. Another example is the investigation of the evolution of the frequency of dry-hot CEs in the Pyrenees under climate change in Lemus-Canovas and Lopez-Bustins (2021), where MBCn was also employed to correct the dependence structure. This revealed more frequent compound hot and dry events in the future. Similarly, Olschewski et al. (2024) investigated the evolution of false spring events (an earlier than average warming event followed by another period of freezing temperatures) and heat-drought CEs in the greater Mediterranean region for a high-impact future scenario, through the MBCn method (Cannon, 2018). Once again, their results show a potential increase in frequency, as well as in intensity and duration for the heat-drought CEs. In Kim et al. (2023a), the representation of four CEs in a Regional Climate Model (RCM) with boundary conditions from a Global Climate Model (GCM) is assessed and compared to the representation of the same events with the boundary conditions corrected through univariate BC and multivariate BC. The used BC methods allow to correct persistence biases and physical inconsistencies between the variables on multiple timescales: they are introduced in Mehrotra and Sharma (2015) and their implementation is detailed in Kim et al. (2023b). They showed that the RCM with multivariate bias corrected

https://doi.org/10.5194/egusphere-2026-3269
Preprint. Discussion started: 19 June 2026

boundary conditions exhibited lower errors in reproducing the CEs frequency and magnitude than the other RCMs (i.e., without correction or with univariate correction).

Benefits and shortcomings of multivariate BC methods are assessed in François et al. (2020) and in Allard et al. (2025), but they do not focus on their ability to correct extreme quantiles and asymptotic dependence. Moreover, there is a lack of understanding about the ability of multivariate BC methods to preserve the signal of climate change for CEs. Therefore, this work addresses two research questions, under the prism of two CEs. First, it investigates whether BC methods enhance the realism of the representation of these two compound events. In this context, the representation of these events in raw climate outputs is evaluated and the influence of BC methods on their representation is analyzed. Second, the study examines the extent to which BC methods preserve the climate change signal of raw climate simulation outputs for these compound events. Indeed, although climate simulations exhibit statistical biases, they remain the most comprehensive tools for understanding the evolution of the Earth's climate system. It is thus essential that BC techniques preserve the physically plausible evolution of climate variables under future scenarios. Following the conclusions of François et al. (2020) and Allard et al. (2025), this study examines two multivariate BC methods, dOTC and R^2D^2, as well as the univariate CDF-t method as a benchmark to put in perspectives the contribution of the multivariate BC methods.

These three BC methods (CDF-t, dOTC and R^2D^2) are compared in an extreme value framework to assess the effectiveness of correcting the dependence structure in the tails of the distribution and the impact of multivariate BC methods on the estimation of compound event probabilities under current and projected climate scenarios. The performance of these methods is assessed using two extremal statistics: the coefficient of extremal dependence χ and the bivariate return period RP. The coefficient of extremal dependence χ (Joe, 1993; Coles et al., 1999) allows to characterize the extremal dependence structure and to compare such structures. The return period RP (Gumbel, 1941) is a natural statistic to characterize an extreme event and the bivariate version encapsulates both the marginal exceedance probabilities and the joint exceedance probability. Estimation of these statistics requires advanced statistical modeling: two different modelings are detailed and used with raw and bias-corrected data. Both are based on the theory of multivariate extreme values. The first one, named the bi-GPD modeling, relies on bivariate Generalized Pareto Distribution (GPD) and is efficient when the variables are asymptotically strongly dependent (Jacquemin et al., 2026). The second one, named the GPD-copula modeling, uses copulas to model the dependence structure and is efficient when variables are asymptotically weakly dependent (Jacquemin et al., 2026). To evaluate the BC methods, χ and RP are computed over reference data, raw simulation data and corrected simulation data. Their comparison permits to discuss the realism of the representation of CEs in simulations as well as the improvement of this representation by BC methods. The temporal evolutions of the same statistics over future periods are also compared to determine whether the trends are preserved or not by BC methods.

This article is organized as follows: in Section 2, the two CEs considered and the data used are presented in details. The BC methods applied and compared in this article are briefly reminded in Section 3. The statistical modelings used to represent the CEs are presented in the same Section, as well as the evaluation statistics: the coefficient of extremal dependence χ and the bivariate return period RP. The experiments conducted in this study are detailed in Section 4. They aim at answering whether BC methods improve the realism of the representation of the two CEs under study in climate simulations and whether

https://doi.org/10.5194/egusphere-2026-3269
Preprint. Discussion started: 19 June 2026

BC methods preserve the climate change signal from the climate simulations in the same two CEs. Results are presented, commented and discussed in Section 5. Section 6 provides conclusions and perspectives of future works.

2 Data and events

This Section presents the reference data and the simulation data used to compare and evaluate the BC methods. Then, the two compound events under study are detailed. They both stroke Europe in the last 10 years. The first event occurred over central France during spring 2016 and is referred to as the Seine/Loire event in the following. The second event is the major flooding of the Ahr river in July 2021 and is called the Ahr event. Finally, the Antecedent Precipitation Index (API), a variable used in the modeling of the events, is introduced.

2.1 Reference and simulation data

Reference data used in this article are daily precipitation time series from ERA5 reanalysis (Hersbach et al., 2020) initially provided at a 0.25° x 0.25° spatial resolution. Ten climate simulations from CMIP6 are considered for correction and are presented in Table 1. For all simulations the considered scenario is SSP 5-8.5, the scenario with the highest radiative forcing (O'Neill et al., 2016). All data (ERA5 and CMIP6 simulations) have been re-gridded to a common 1°x 1° spatial resolution.

Simulation name	Run	Atmospheric resolution	Data reference
BCC-CSM2-MR	r1i1p1f1	∼100 km	Wu et al. (2018)
CanESM5	r10i1p1f1	∼500 km	Swart et al. (2019)
CNRM-CM6-1	r1i1p1f2	∼250 km	Voldoire (2023)
CNRM-CM6-1-HR	r1i1p1f2	∼100 km	Voldoire (2019)
CNRM-ESM2-1	r1i1p1f2	∼250 km	Seferian (2023)
INM-CM4-8	r1i1p1f1	∼100 km	Volodin et al. (2019)
INM-CM5-0	r1i1p1f1	∼100 km	Volodin et al. (2019)
IPSL-CM6A-LR	r14i1p1f1	∼250 km	Boucher et al. (2018)
MIROC6	r1i1p1f1	∼250 km	Shiogama et al. (2019)
MRI-ESM2-0	r1i1p1f1	∼100 km	Yukimoto et al. (2019)

Table 1. List of CMIP6 simulations used in this study, along with their run, approximate horizontal atmospheric resolution, and associated reference.

2.2 The Seine/Loire 2016 event

Spring 2016 was particularly wet in France (Philip et al., 2018). On top of that, an almost stationary low pressure system created moderate but continuous rain from 26 May to 4 June 2016 over Central and North-East France. This resulted in the flooding of first small tributary rivers, like the Loing and the Yvette, and then in the almost simultaneous flooding of two major french

https://doi.org/10.5194/egusphere-2026-3269
Preprint. Discussion started: 19 June 2026

rivers, the Seine and the Loire (Philip et al., 2018). This extreme event can be seen as a spatially compound event (Zscheischler et al., 2020). River discharge, the classical variable to represent floodings, is however not an output of climate simulations. In order to exploit climate simulations, the Seine/Loire event is represented by climate variables such as precipitation. It can be shown that the daily precipitation values from 26 May to 4 June 2016 were not extremes *per se*, but that the accumulated precipitation of the last 20 days of May 2016 was exceptionally high.

To characterize this event, the precipitation variable from the data presented earlier is used. The watershed of the Seine and the watershed of the Loire are discretized over the 1°x 1° re-gridded ERA5 grid. The are presented on panel (a) of Figure 1, in green for the watershed of the Seine and in red for the watershed of the Loire. The daily precipitation data is then averaged over each watershed.

2.3 The Ahr 2021 event

On 11 July 2021, an upper-level low pressure system formed west of Ireland. It moved eastward across Europe, before being blocked by a quasi-stationary anticyclone located over northeastern Europe, already present during the 3 preceding weeks. This anticyclone has led to sea surface temperature anomalies up to 8K over the Baltic sea (Mohr et al., 2023). In the meantime, a surface low-pressure system arrived from northwestern Italy. It all resulted in very high values of precipitation over northern Germany on the 14 and 15 of July 2021. It also resulted in the flooding of the Ahr catchment, a river between Belgium and Germany, and in never seen before precipitation for this area. However, as analyzed in Mohr et al. (2023), the soil moisture level in the Ahr catchment before this extreme rainfall was high and played a decisive role in the disastrous flood. In this work, the Ahr event is considered a preconditioned event (Zscheischler et al., 2020), with the high soil moisture level being the preconditioning variable and the daily precipitation being the main variable.

To characterize the Ahr event, the precipitation is also used. The grid cell corresponding to the flooded area is retained as well as the eight surrounding grid cells. The 3°x 3° retained area is shown on panel (b) of Figure 1. The daily precipitation data is then averaged over this area.

2.4 The Antecedent Precipitation Index

To account for the accumulation of precipitation, the relevant variables for the Seine/Loire event, the Antecedent Precipitation Index (API) is used in this study. The API, introduced by Kohler and Linsley (1951), corresponds to accumulated precipitation with the natural evacuation of water by the watershed. Moreover, to statistically model the Ahr event, the soil moisture variable presents two drawbacks: it is not an output of climate simulations and it is bounded. The upper bound (which represents the saturation of the soil in water) strongly limits the use of this variable in an extreme event study, as no distinction between high values and extreme values can be made. To overcome both problems, the API is also used for the Ahr event to describe the wetness conditions prior to the heavy rainfall, as in Mohr et al. (2023).

On a day j, the API is defined by:

$$API_j = \sum_{i=1}^{m} k^{i-1} PR_{j-i}, \tag{1}$$

https://doi.org/10.5194/egusphere-2026-3269
Preprint. Discussion started: 19 June 2026

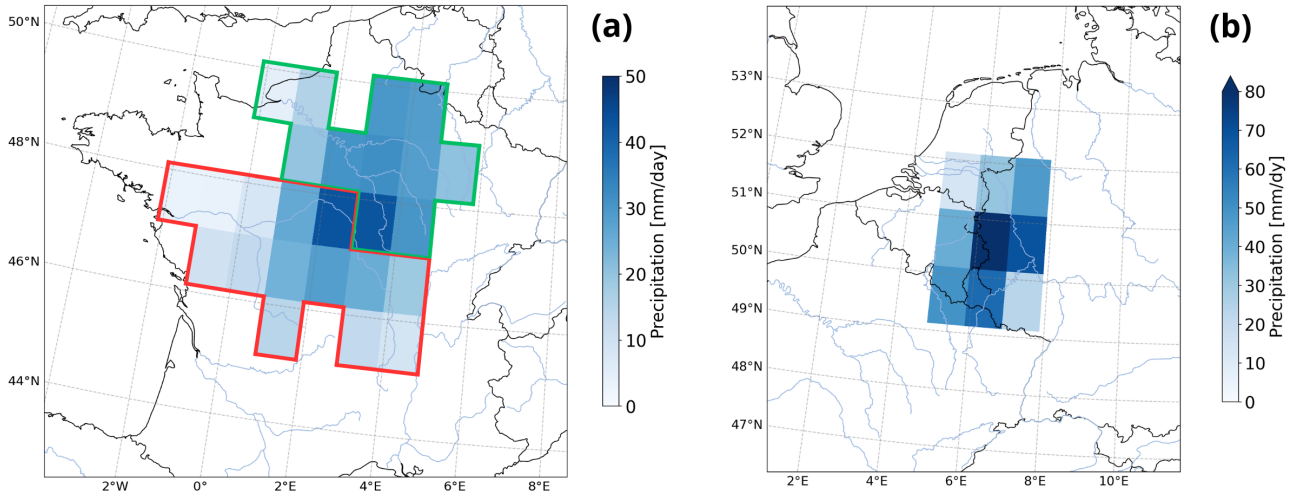

Figure 1. Seine (green) and Loire (red) watersheds on a 1°x 1° grid with precipitation on the 31/05/2016 (a). Selected area for the Ahr event with precipitation of the 14/07/2021 (b).

where PR_d is the total precipitation at day d. The value of the API depends on two parameters, k and m. The number of days used to calculate the API is given by m and k accounts for the evacuation of the water by the watershed.

For the Seine/Loire, similarly as in Jacquemin et al. (2026), we set $m = 17$ and $k = 0.87$ for both watersheds. These values come from the literature (Blanchard et al., 1981; Li et al., 2021) and from a model stability analysis (not shown). The maxima of API reached on May-June 2016 are 39.6 mm for the Seine and 41.1 mm for the Loire.

For the Ahr event, parameters $m = 30$ and $k = 0.9$ are chosen: they are within the suggested bounds of the literature (Blanchard et al., 1981; Teng et al., 1993; Schröter et al., 2015; De Moraes et al., 2024) and were used in Mohr et al. (2023) to analyze the Ahr event. An analysis (not shown) also showed that the API with this set of parameters follows the variations of the soil moisture in ERA5 in the upper soil levels (0-28 cm) without being bounded. The maximum of precipitation was reached on the 14th of July 2021 and the retained value for the API is on the same day, as the precipitation of the day is not included in the calculus of the API (see Eq. (1)). The maximum value of precipitation is 46.6 mm and the corresponding API value is 64.4 mm.

3 Methodology

First, the BC methods employed in this article are introduced: CDF-t, R^2D^2 and dOTC. Then, the two statistical modelings used to compute relevant statistics about the events under study are presented, as well as the practical estimation methods. Finally, the extremal statistics over which the comparison of the BC methods is done are presented, as well as the formulas to compute them from the two statistical modelings.

https://doi.org/10.5194/egusphere-2026-3269
Preprint. Discussion started: 19 June 2026

3.1 Bias correction methods

CDF-t

The "Cumulative Distribution Function - transform" (CDF-t) is a univariate BC method, introduced in Michelangeli et al. (2009). This BC method is used in many studies, such as Pierce et al. (2015); Famien et al. (2018); Guo et al. (2020); Vrac et al. (2025). Over the calibration period, the method learns the modification needed to transform the Cumulative Distribution Function (cdf) of the climate simulations into the cdf of the reference time series. It then learns the evolution of the simulation cdf between the calibration period and the projection period. This evolution is assumed to be the same for the reference cdf between the two periods. By combining the transformation and the evolution previously learned, CDF-t constructs the corrected cdf over the projection period. Finally, a simple quantile-mapping is performed between the newly constructed cdf and the cdf of the time series of the climate simulation over the projection period, to obtain the bias-corrected time series. CDF-t has the advantage over the classic quantile-quantile method to take into account the evolution of the cdf of the simulation between the calibration period and the projection period. A complete description can be found in Vrac et al. (2012); François et al. (2020).

dOTC

The dynamical Optimal Transport Correction (dOTC) was introduced in Robin et al. (2019). It places the "quantile-mapping" transfer function in the context of the optimal transport theory. The optimal transport theory defines the optimal way to transform one distribution into another one. This transformation function is called an optimal transport plan. In dOTC, two optimal plans are inferred: the first one between simulation data and reference data over the calibration period and the second one between simulation data over the calibration period and simulation data over the projection period. Finally, the two optimal transport plans are combined to construct the multivariate cdf of the corrected data over the projection period. By taking into account the evolution of the climate simulation's cdfs between the calibration and the projection periods in a manner similar to CDF-t, dOTC is the extension of CDF-t to the multivariate case (Robin et al., 2019).

R^2D^2

The Rank Resampling for Distributions and Dependences (R^2D^2), presented by Vrac (2018), first corrects the marginal distributions with a univariate BC method (such as CDF-t), then corrects the dependence structure, and finally combines the two steps to provide a multivariate correction. The dependence structure is corrected based on the Schaake Shuffle, described in Clark et al. (2004). It consists in reordering a sample so that its rank structure matches the rank structure of a reference sample. For R^2D^2, a "pivot" needs to be selected i.e., a variable whose rank chronology will not be modified. Selecting different variables as pivot allows to bring variability in the timing of the events. Hence, R^2D^2 reconstructs the inter-variable correlation of the reference data while keeping the rank chronology of the pivot variable (and changing the rank chronology of the other variables). By construction, R^2D^2 assumes the reference inter-variable dependence structure to be stationary. A variation of R^2D^2 was introduced in Vrac and Thao (2020) in which temporal correlation is also taken into account. This version of R^2D^2

https://doi.org/10.5194/egusphere-2026-3269
Preprint. Discussion started: 19 June 2026

reconstructs the inter-variable correlation by conditioning the rank resampling on the pivot variable at lagged time steps. The first version is named R^{2}D^2_NTC (No Temporal Correlation) in this article to differentiate it from the second version of R^{2}D^2 that takes temporal correlation into account. The latter is the selected version in this article, whereas the former is used only in Section 5.5 to focus on the preservation of the temporal correlation by BC methods.

Note that R^{2}D^2 can also be applied with a multivariate pivot (e.g., the two variables of interest). The use of a multivariate pivot was tested but not retained for this study, due to the absence of a clear improvement of the results compared to the use of a univariate pivot (not shown). In this article, R^{2}D^2 can be used twice for each event, once with each variable as the pivot variable. To facilitate reading, only the API of the Seine for the Seine/Loire event and the precipitation for the Ahr event are retained as the pivot for R^{2}D^2 in the following.

3.2 Statistical methodology for bivariate extremes

To compare BC methods and assess their impacts on the representation of compound events, two statistics are selected: the coefficient of extremal dependence χ and the bivariate return period RP. Both are presented below. An appropriate statistical representation of the bivariate extremes that define the compound event is required for both statistics to be as accurate as possible. Hence, two bivariate extremal modelings are presented in this Section. Each modeling has its own strengths and weaknesses, as established in Jacquemin et al. (2026).

In the following, the bold notation corresponds to vectors. Let us note F the cdf of $\boldsymbol{X} = (X_1, X_2)$, a bivariate random stationary process indexed over time, and F_i the marginal cdf of X_i, $i = 1, 2$. For $x_i \in \mathbb{R}$, the cdf of X_i is denoted $F_i(x_i) = \mathbb{P}(X_i \leq x_i)$ and the bivariate cdf of $\boldsymbol{X}$ is $F(x_1, x_2) = \mathbb{P}(X_1 \leq x_1, X_2 \leq x_2)$. We further denote $\bar{F}$ the joint survival function defined by $\bar{F}(x_1, x_2) = \mathbb{P}(X_1 > x_1, X_2 > x_2)$ and the marginal survival function $\bar{F}_i = 1 - F_i$ for $i = 1, 2$. In the following, the maximum of a vector and inequalities between vectors are meant component-wise.

Statistical modelings

Following the conclusions in Jacquemin et al. (2026), the bi-GPD modeling is chosen to represent the Seine/Loire event. The bi-GPD modeling relies on multivariate Generalized Pareto distribution, introduced in Rootzén and Tajvidi (2006) and characterized in Rootzén et al. (2018). The modeling is presented in details in Jacquemin et al. (2026) and summarized here for sake of completeness. This modeling requires an expression for the whole marginal distributions, not only for the tails. In this work, the Extended Generalized Pareto Distribution (EGPD) presented by Naveau et al. (2016) is chosen to model the univariate distributions while ensuring a tail behavior similar to that of a GPD. Using the fitted EGPD, the two marginals are then transformed to follow a unitary exponential distribution.

The vector $\boldsymbol{Z} = (Z_1, Z_2)$, defined by the exceedances of both unitary exponentials above a high bivariate threshold $\boldsymbol{u} = (u_1, u_2)$, follows a unitary bivariate GPD. Then, according to Rootzén et al. (2018), there exists a random vector $\boldsymbol{T} = (T_1, T_2)$ such that $\boldsymbol{Z}$ and $E + \boldsymbol{T} - \max(\boldsymbol{T})$ are equal in distribution, with E being a unitary exponential random variable independent from $\boldsymbol{T}$. The random variable Δ has been introduced by Legrand et al. (2023) with $\Delta = Z_1 - Z_2 = T_1 - T_2$. From this, it

https://doi.org/10.5194/egusphere-2026-3269
Preprint. Discussion started: 19 June 2026

was shown in Jacquemin et al. (2026) that the joint excess probability beyond the high bivariate threshold $\boldsymbol{u}$ can be expressed non-parametrically, mobilizing the empirical cdf of Δ and numerical integration.

Following the conclusions in Jacquemin et al. (2026), the GPD-copula modeling is chosen to represent the Ahr event, as the bi-GPD modeling is unable to correctly represent asymptotically independent events. The GPD-copula modeling first relies on a modeling of the tails of the marginal distribution. The univariate extreme value theory states that, under some conditions, the distribution of exceedances over a high threshold can be approximated by a GPD (Beirlant et al., 2006): for a threshold u_i for $i = 1, 2$ such that $F_i(u_i) = p$ is close to 1, the function $\mathbb{P}(X_i \leq \cdot \mid X_i > u_i)$ is approximately a GPD.

To represent compound events, the dependence structure in the extremes must also be accounted for. According to Sklar's theorem (Sklar, 1959), there exists a function $C : [0,1]^2 \to [0,1]$ called the copula of $\boldsymbol{X}$ defined for all $\boldsymbol{x} = (x_1, x_2) \geq 0$ such that $F(x_1, x_2) = C(F_1(x_1), F_2(x_2))$. Let us suppose that F is in the domain of attraction of a bivariate extreme value distribution, which implies that the margins of F are in the domain of attraction of a univariate extreme value distribution, or equivalently, that their exceedances over a high threshold can be approximated by a GPD (Beirlant et al., 2006). Then, applying Sklar's theorem to the function of the bivariate exceedances, there exists a copula function characterizing the dependence structure in the extremes. The combination of the GPD modeling for the univariate extremes and the copula for the joint exceedances leads to the GPD-copula modeling.

Estimation of the parameters

For the GPD-copula modeling, the GPD parameters are estimated using Maximum Likelihood Estimation (MLE) and the R package *tea* (Ossberger, 2020). A threshold u_i of probability $p = 0.95$ is chosen for each margin. The parameters of the copula are estimated using MLE and the R package *VineCopula* (Nagler et al., 2025).

The copula is chosen among several classical parametric copula families, namely the Independent, Gaussian, Student, and Frank families, as well as the Clayton, Gumbel and Joe families with their $90°$, $180°$ and $270°$ rotations (see Nagler et al. (2025) for more details). The Bayesian Information Criterion (BIC) is used to select the best copula family, averaged over quantiles ranging from the 0.90 to the 0.98 probability levels, with a lag of 0.01. The BIC is set to 0 if the association (positive or negative) at a certain probability level is different from the association at the 0.95 probability level. Moreover, to bring stability to the copula family selection process, the Gumbel copula is chosen if the difference between the averaged BIC corresponding to the Gumbel and that of the selection process is less than 2 units. This whole process is intended to get a more robust copula family selection, as an arbitrary threshold may not lead to the best representation of the high level dependence structure. It brings stability, as the Gumbel is often chosen, but also discrimination, as a difference in copula family is generally linked to a significant difference in the dependence structure. The limit of 2 BIC units is chosen based on the work of Kass and Raftery (1995), in which they show that models with less than 2 BIC units of difference are indiscernible. Finally, the Gumbel copula is the preferred copula in case of indiscernibility as it is the only extreme value copula in the previously mentioned families.

The parameters of the EGPD are estimated using MLE and the *mev* package (Belzile [aut et al., 2024), modified to allow $\xi > -0.5$. Other parameters not mentioned in this article are estimated similarly as in Jacquemin et al. (2026). More details are given in Appendix A.

https://doi.org/10.5194/egusphere-2026-3269
Preprint. Discussion started: 19 June 2026

3.3 Extremal statistics used for evaluation

The first statistic used to compare the three BC methods is the coefficient of extremal dependence (Joe, 1993), defined as $\chi = \lim_{v \to 1} \chi(v)$, with $\chi(v) = \mathbb{P}(F_2(X_2) > v \mid F_1(X_1) > v)$. Here, we use $\chi \simeq \chi(v)$ with $v = 0.9999$. Clearly, $\chi \in [0,1]$. The upper limit, $\chi = 1$, corresponds to perfect asymptotic dependence, whereas $\chi = 0$ corresponds to asymptotic independence. The value of $\chi \in (0,1)$ gives a measure of the strength of the asymptotic dependence.

The coefficient of extremal dependence can be expressed with both statistical modelings. It can be expressed in terms of the copula, since $\chi(v) = 2 + (C(v,v) - 1)/(1-v)$ with $v = 0.9999$. With the bi-GPD modeling, the coefficient of extremal dependence is expressed by $\chi(v) = \bar{F}(u_1, u_2)/(1-p)$ (Jacquemin et al., 2026). Note that in this case $\chi(v)$ is independent of v conditionally on $v \geq p$, with $p = F_1(u_1) = F_2(u_2)$ and (u_1, u_2) the high bivariate threshold in the construction of Δ.

The second statistic used to compare the BC methods is the bivariate return period RP. Here, a univariate extreme event is defined as the exceedance of a random variable X above an extreme value x_{RP} named the "return level". For a bivariate compound event (in our case, either a spatially CE or a preconditioned CE), the definition becomes that each variable X_i exceeds its respective return level $x_{RP,i}$ at *relatively close times*. The notion behind *relatively close times* is discussed in details in Jacquemin et al. (2026). Here, closeness is set to 4 days for the Seine/Loire event and 7 days for the Ahr event. A sensitivity analysis revealed that our results did not change qualitatively when increasing this interval (Jacquemin et al., 2026). The return period RP is then defined as the expected time between two such events. The complete expressions for RP with each modeling (the GPD-copula and the bi-GPD) can be found in Jacquemin et al. (2026), along with their mathematical derivation. They are not detailed in this work because they require the introduction of statistical notions that are not of interest here. The key element to note is that the return period RP requires estimating the probability $\bar{F}(\boldsymbol{x}_T) = \mathbb{P}[X_1 > x_{RP,1}, X_2 > x_{RP,2}]$. This probability is estimated with either the GPD-copula or the bi-GPD modeling.

4 Design of experiments

For both the Seine/Loire and the Ahr events, the numerical experiments are the same. The calibration period is chosen to be 1992-2021. The 2022-2100 time period is cut into three 30-year projection periods: 2022-2051, 2041-2070, and 2071-2100. The Seine/Loire event occurred in early June 2016, so only the values of API for the months of May and June are considered. For the Ahr event, only the summer months (June, July, and August) are considered. The statistical modelings described previously are applied to compute the two extremal statistics of interest: the bi-GPD modeling for the Seine/Loire event and the GPD-copula modeling for the Ahr event.

4.1 Evaluation of the bias correction methods

To evaluate the BC methods, we first propose an experiment that permits to assess whether the two extremal statistics of interest are statistically well represented in the raw and in the bias corrected climate simulations. This evaluation takes place over the calibration period 1992-2021. A common 2-fold procedure is applied: data are separated into two subsets of 15 years,

https://doi.org/10.5194/egusphere-2026-3269
Preprint. Discussion started: 19 June 2026

either randomly or sequentially. These experiments are referred to as “random 2-fold” and “sequential 2-fold" experiments, respectively. For the sequential 2-fold experiment, the subset covering 1992-2006 is used for training the BC methods, and the other one covering 2007-2021 is used for evaluation. For the random 2-fold experiment, the two subsets of 15 years each are drawn randomly without replacement. Then, the roles of the subsets are inverted: the previous evaluation subset is now used for training while the previous training subset is now used for evaluation. Finally, the two 15-year corrected subsets are joined to reconstruct a 30-year corrected version of the original dataset. These experiments are represented in Figure 2, with the random split in panel (a) and the sequential split in panel (b). To create confidence intervals, the corrected dataset of size 30 years is then bootstrapped: it is realized by sampling years in order to preserve the temporal dynamic of the API variables. The whole sequence i) construction of the subsets, ii) bias correction, iii) merging of the corrected subsets, iv) bootstrapping, v) computation of the extremal statistics (RP and χ) is repeated 100 times. The bootstrap step in iv) allows us to assess the uncertainty of the estimation.

Some remarks can be made concerning these experiments. No BC method is applied to ERA5 and to the raw climate simulations. In this case, these experiments boil down to a classical bootstrap for establishing a variability interval. In the case of the sequential 2-fold experiment, the split is always the same. Therefore, the variability arises only from the 100 bootstrap samples. In the case of the random 2-fold experiment, the variability comes both from the random split and from the bootstrap.

Within the sequential experiment, the distributions of the two subsets may not be similar because an evolution occurred, potentially due to climate change. With the random split, the distribution of the training subset and that of the evaluation subset are assumed to be equal. In this experiment, the climate is therefore similar in both sets. Applying both experiments allows us to evaluate the BC methods in an ideal stationary context (random 2-fold experiment) and then to evaluate the robustness of the BC methods when a temporal evolution is introduced (sequential 2-fold experiment).

The results are presented in Section 5.2 for the random 2-fold experiment and in Section 5.3 for the sequential 2-fold experiment.

4.2 Bias correction experiment for projection

Based on a second type of experiment, we assess whether BC methods are able to preserve the evolution in time of the extremal statistics. BC methods are now calibrated over the entire period 1992-2021 and applied to each of the three 30-year future periods: 2022-2051, 2041-2070, and 2071-2100. For the raw climate simulations, each statistic is computed for each of the 4 periods, allowing us to determine an evolution over time. For each BC method, the evolution of the corrected climate simulations is also estimated and compared to the raw evolution to determine whether BC methods preserve a climate change signal in the compound events. Similarly to the previous sequential 2-fold experiment, data are bootstrapped 100 times to construct variability intervals. The results are presented in Section 5.4.

https://doi.org/10.5194/egusphere-2026-3269
Preprint. Discussion started: 19 June 2026

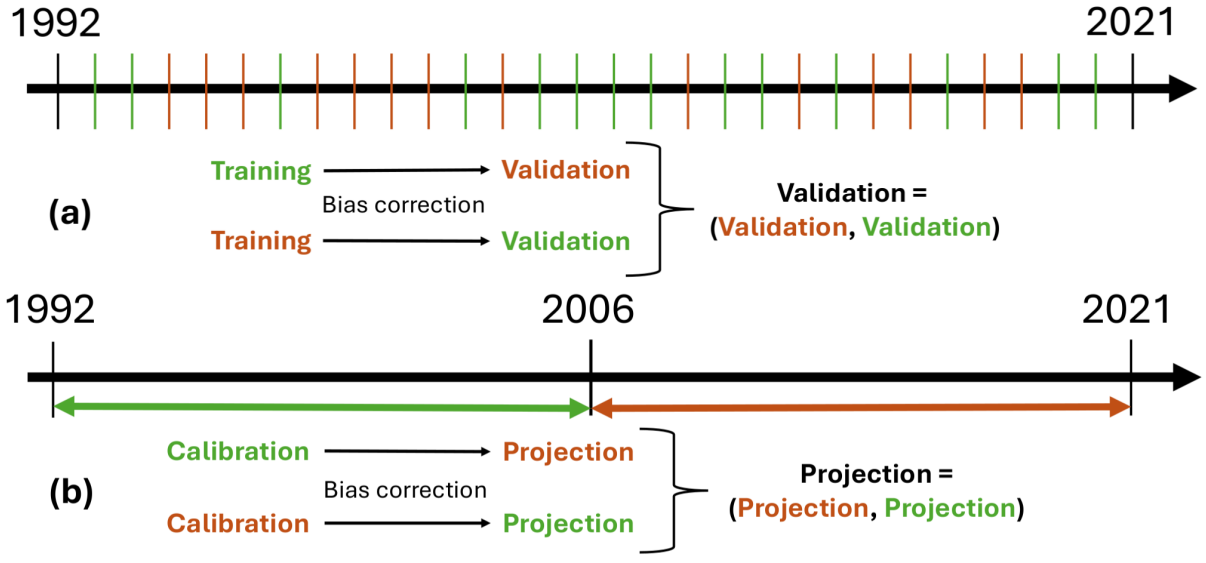

Figure 2. Schematic views of (a) the random 2-fold experiment and (b) the sequential 2-fold experiment.

5 Results

The coefficients of extremal dependence (χ) and the return periods (RP) computed through the experiments described in the previous sections are now presented and analyzed. It may happen that the estimated shape parameter of the GPD or of the EGPD is negative ($\xi < 0$) and that, in the meantime, the return level exceeds the maximum of the support of the distribution (equal to $u_i - \sigma/\xi$). This combination leads to a univariate exceedance probability equal to 0 and therefore to an infinite return period. Extremely high values for the return periods are also possible, say with values above 10^5 years. Since these are not relevant to our study, return periods are from now on censored at 10^5 years in all figures.

5.1 Moving away from the maximum

The initial return levels (one for each variable) of the CEs studied in this work correspond to the maximum of at least one of the variables defining the CE, see Section 2.4. On the climate simulations, the computations described earlier lead often to estimated return periods exceeding 10^5 years and/or to high variability of those, for example because the initial return levels are much larger than the values seen in some simulations. To limit the number of estimated return periods exceeding 10^5 years and also to reduce the variance of the results, it can thus be interesting to move away from the maximum, for instance by considering return levels that are percentages of the initial return levels while still corresponding to extreme quantiles. For simplicity and ease of presentation, the same percentage will be considered for both return levels. Specifically, on the Seine/Loire event, considering 80% of the initial return levels corresponds to a probability $p = 0.997$ on both margins. For the Ahr event, the initial return levels correspond to the maximum observed value for precipitation and to the value of API on the

https://doi.org/10.5194/egusphere-2026-3269
Preprint. Discussion started: 19 June 2026

same day (which is not necessarily the maximum observed API). Considering 80% of the return levels leads to a probability $p = 0.999$ for the precipitation and $p = 0.977$ for the API.

Figure 3 presents return periods for 80%, 90% and 100% of the initial return levels when using the random 2-fold experiment (see Section 4.1). Clearly, when moving away from the maximum, the number of return periods above 10^5 years decreases, as does their variability. For example, for the Seine/Loire event with dOTC bias correction (panel (a)), the inter-quartile range is 99 587 years at 100%, 1 794 years at 90% and 110 years at 80%. Note that, for all percentages, the median and the inter-quartile range are lower for dOTC than for CDF-t for the Seine/Loire event (panel (a) of Figure 3). The order between the median (respectively the inter-quartile range) of CDF-t and the median (respectively the inter-quartile range) of dOTC is preserved by reducing the return levels. This preservation of the order can also be observed between no correction and any other BC method, for both the Seine/Loire and the Ahr events. Figure 3 thus illustrates that moving away from the maximum (but still remaining at extremely high quantile levels) helps to stabilize our results, while preserving the same behavior as at the maximum. From now on, the return levels used to present our results are set to 80% of the initial return levels.

5.2 Evaluation in a stationary context: the random 2-fold experiment

Bias correction methods are first evaluated on their ability to retrieve the ERA5 values of the chosen extremal statistics (χ and RP) in a stationary context, i.e.: they are evaluated on their ability to improve the realism of the CEs in a stationary context, which corresponds to the random 2-fold experience. These two statistics are presented in panels (a) and (c) in Figures 4 and 5 for the Seine/Loire and the Ahr event, respectively, for all combinations "climate simulations (including ERA5) $\times$ correction (including absence of correction)". For each of these combinations, 100 random draws are performed. In all figures, the symbol corresponds to the median value and the vertical bar represents the centered interval containing 95% of the values. The bold dotted red line corresponds to the ERA5 median and the two outer red dotted lines correspond to the 95% variability interval. The gray symbols on the left show the medians obtained with raw climate simulations. Other colors correspond to the bias corrected climate simulations using the random 2-fold experiment described in Section 4.1. Recall that estimated RP above 10^5 are censored to that value.

A nonparametric paired difference test is performed to test whether the mean of a statistic computed on the reference data and the mean of the same statistic computed on climate simulations are equal or not. Specifically, on each bootstrap sample of the pair (reference, climate simulation), the difference between the two statistics is computed. The difference is made between the values for χ and, in order to bring numerical stability, between the logarithm of the values for RP. A 95% variability interval is constructed from this set of differences. The null hypothesis "H_0: the expectations of the two statistics are equal" is rejected if 0 is outside this variability interval. One can refer to Xu (2006) for more details on this statistical test. On each combination of climate simulation and bias correction, a star symbol on the top or the bottom of the error bars indicates that H_0 has been rejected.

First, let us consider the Seine/Loire event (Figure 4). For the coefficient of extremal dependence χ (panel (a)), H_0 is rejected for one raw climate simulation (CNRM-CM6-HR) only. Even though the raw BCC median is lower than the raw CNRM-CM6-HR median, the statistical test focuses on the mean and not on the median, which may explain why H_0 is not rejected for BCC.

https://doi.org/10.5194/egusphere-2026-3269
Preprint. Discussion started: 19 June 2026

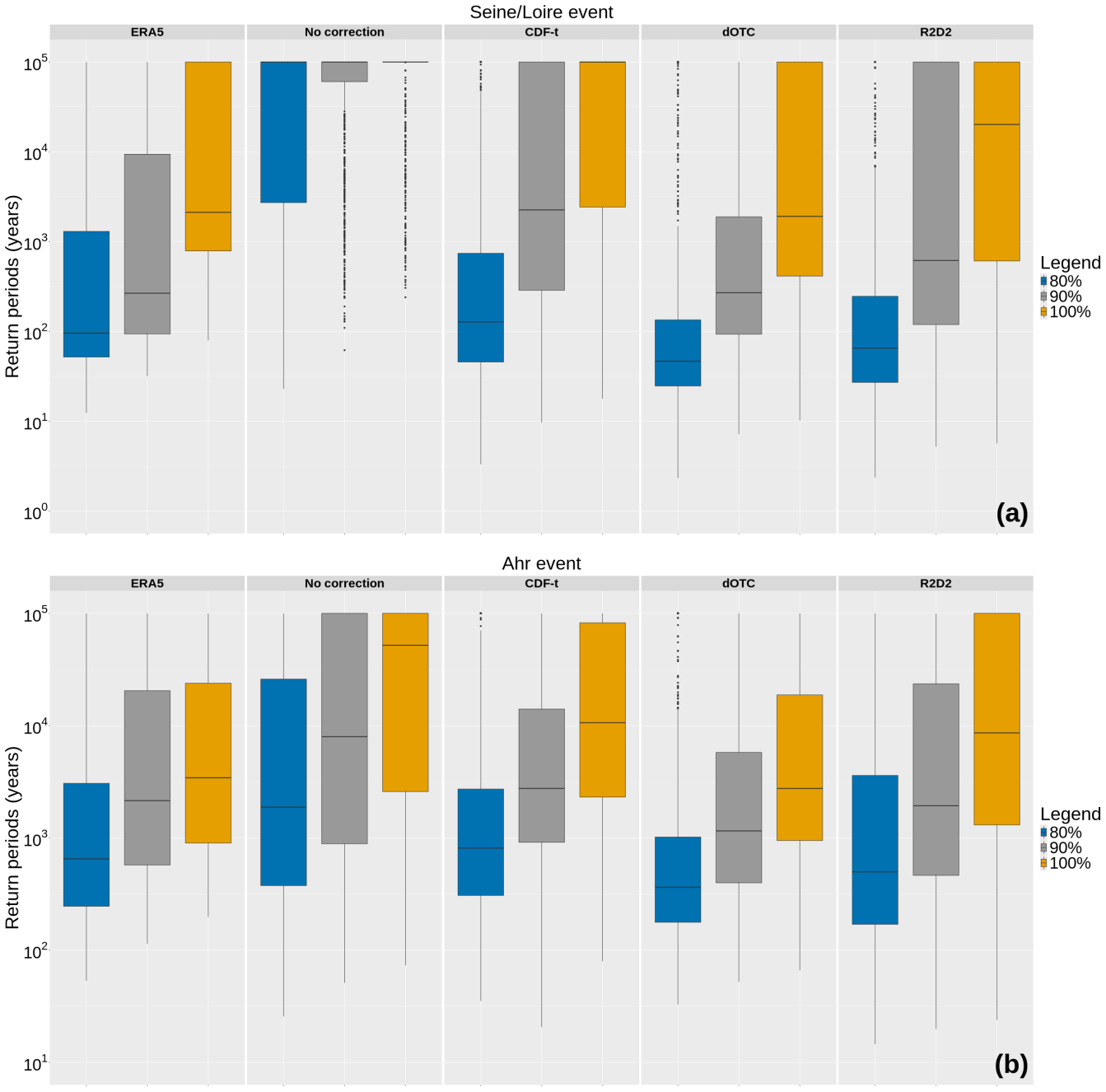

Figure 3. Return periods for the Seine/Loire event (a) and for the Ahr event (b) with 80%, 90% and 100% of the maximum observed values. The boxplots pool all values computed from the 100 random 2-fold draws for ERA5 and for the 10 climate simulations. Values above 10^5 are censored to that threshold.

https://doi.org/10.5194/egusphere-2026-3269
Preprint. Discussion started: 19 June 2026

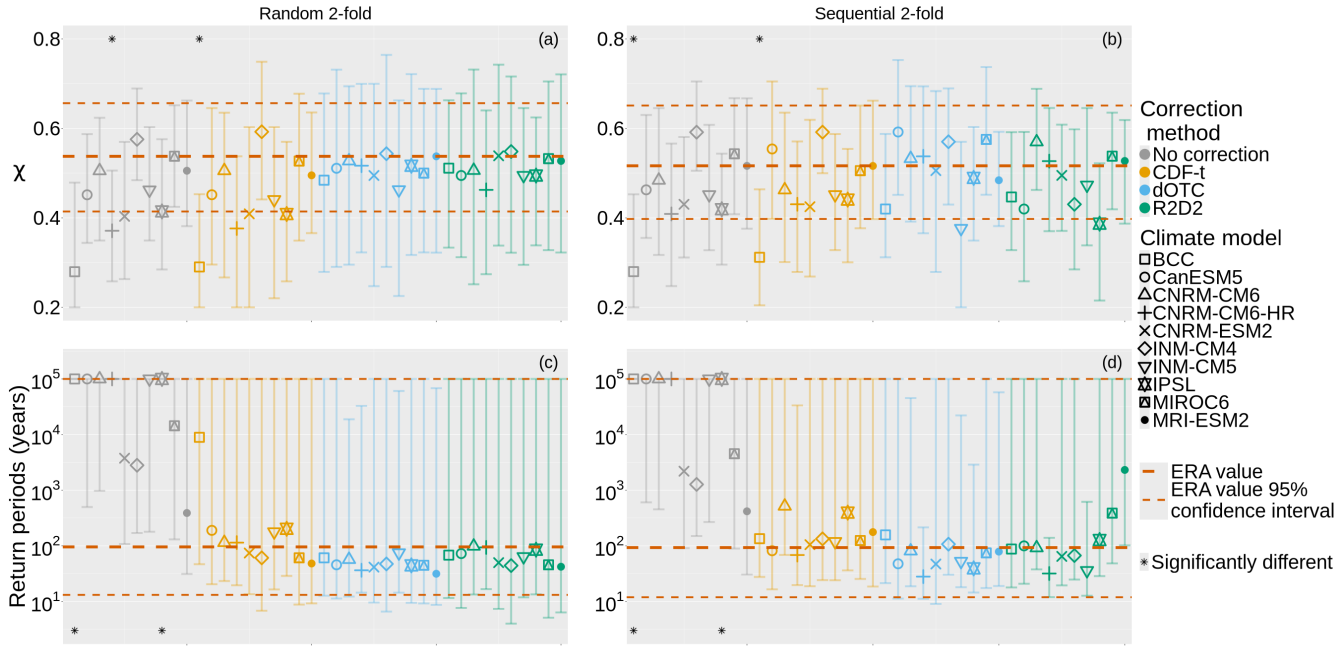

Figure 4. Coefficient of extremal dependence χ (a, b) and bivariate RP (c, d) for the Seine/Loire event; Results of the random 2-fold experiment (a, c) and of the sequential 2-fold experiment (b, d). See details in Section 4.1.

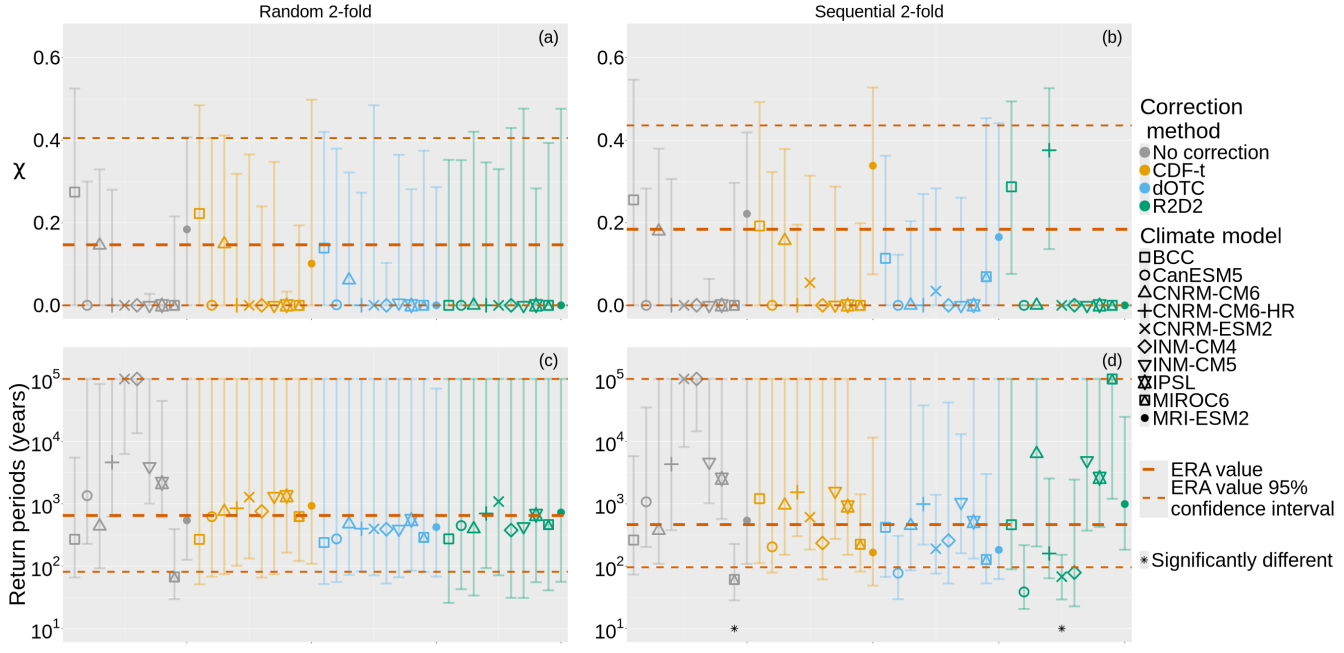

Figure 5. Similar to Figure 4 but for the Ahr event.

https://doi.org/10.5194/egusphere-2026-3269
Preprint. Discussion started: 19 June 2026

Among the BC methods, CDF-t is in theory expected not to modify the dependence structure and therefore to exhibit χ values equal to those of the raw simulations. However, with the bi-GPD modeling, χ is estimated using a frequency estimator and is therefore determined by the number of points in the upper-right area (see Section 3.3). Within the 2-fold experiment, the number and the positions of the points in the upper-right area of a bivariate distribution may change from one random sample to another. The sampling procedure therefore modifies the estimate of χ, resulting in a variability usually absent when correcting with CDF-t. However, these differences remain limited: among all climate simulations, only the values from BCC are significantly different from the ERA5 baseline and the values from CNRM-CM6-HR are not significantly different anymore from the ERA5 baseline, despite little visual differences with the raw climate simulation. R^2D^2 and dOTC both return χ values closer to the ERA5 baseline than those of the uncorrected simulations. There are no significant differences and all variability intervals overlap the ERA5 variability interval. This correction of the χ values is due to the correction of the dependence structure by the multivariate BC methods.

For the return period RP (Figure 4, panel (c)), the situation is dramatically different on the raw climate simulations. Even though H_0 is rejected only for two uncorrected climate simulations (BCC and IPSL), for 6 of them (out of 10) the medians of the estimated return periods are larger than 10^5 years. Note that the variability interval for ERA5 is huge, from 10 years to 10^5 years. Indeed, for both API variables, the most extreme values in ERA5 data are only reached during the year 2016. During the bootstrap step, it is possible that some samples do not contain the year 2016, which implies that even 80% of the maximum values are highly unlikely for such samples, hence the huge variability. All BC methods improve the estimation of the return periods for all the climate simulations: the medians are closer to the ERA5 median, the variability intervals overlap the ERA5 variability interval and H_0 is not rejected for any simulation. It can be noted that BCC with CDF-t exhibits a median 100 times higher than the ERA5 median (although not significantly different), which can be explained by strongly biased χ values. Without correction, BCC presents χ values that are the furthest away from the ERA5 values and those are almost not modified by CDF-t. In addition, for BCC the CDF-t corrected median of χ is equal to 0.29, closer to asymptotic independence ($\chi = 0$) than the ERA5 median, which is equal to 0.54. Moving towards asymptotic independence increases the return periods, thus explaining the gap between BCC return periods corrected by CDF-t and those of the other climate simulations, also corrected by CDF-t.

Similar observations can be made for the Ahr event, presented on panels (a) and (c) of Figure 5. For the coefficient of extremal dependence χ (panel (a)), no climate simulations reject H_0 and the majority of them present a median χ value of 0. Only 3 raw climate simulations (out of 10) have a median value different from 0. Note that the estimated χ value with the ERA5 data is equal to 0, thus multivariate BC methods try to correct the climate simulations towards this value. CDF-t brings some variability in the estimated values but no major changes in the medians are observed. The three climate simulations with medians different from 0 are brought closer to 0 by dOTC and MRI-ESM2 even has a median equal to 0. R^2D^2 leads to an even stronger correction, all medians being equal to 0. Even though the χ values are mostly correct for the raw climate simulations, the multivariate BC methods improve the realism of the extremal dependence coefficients.

Regarding RP (Figure 5, panel (c)), one must first acknowledge that the variability interval for ERA5 goes from 10^2 years to 10^5 years. On raw simulations, H_0 is never rejected even though for two simulations (CNRM-ESM2 and INM-CM4) the

https://doi.org/10.5194/egusphere-2026-3269
Preprint. Discussion started: 19 June 2026

median is above the 10^5 years limit and for MIROC6 the median is below the lower limit of the ERA5 interval. For all BC methods, the median of the estimated return periods gets closer to the ERA5 median, usually between the median and the lower end of the variability interval. H_0 is never rejected. In almost all cases, the upper end of the variability interval is above 10^5. This can be explained by the nature of the Ahr event, characterized by two asymptotically independent variables. Furthermore, the GPD-copula modeling shows a high variability because the estimation of the copula parameters is sensitive to the low number of points resulting from the bootstrap (see Jacquemin et al., 2026, for more details).

In conclusion, multivariate BC methods lead to improved estimations of two important extremal statistics, the coefficient of extremal dependence χ and the return period RP, in a stationary context. Among the tested BC methods, CDF-t requires a correct dependence structure prior to the correction in order to provide an accurate estimate of RP, which is expected by construction of CDF-t.

5.3 Evaluation in a non-stationary context: the sequential 2-fold experiment

In contrast to the previous experiment, the sequential 2-fold experiment described in Section 4.1 brings some non-stationarity. Comparing the results in this non-stationary context to the ones in the stationary context (see previous Section) allows us to assess the impact of non-stationarity on the bias correction. On Figures 4 and 5, panels (b) and (d) can hence be compared to panels (a) and (c) for χ and RP respectively. Notice that in this experiment, contrarily to the previous one, the data-set is always partitioned into two calibration [1992-2006] and evaluation sets [2007-2021]. The variability in the estimates is thus only due to the bootstrapping step. As a consequence, the medians and variability intervals on ERA5 and on the raw simulations are slightly different than those obtained with the random 2-fold experiment. The same nonparametric statistical test than in the previous Section is performed: the null hypothesis "H_0: the expectations of the two statistics are equal" is rejected if 0 is outside the variability interval of the differences.

We start with the Seine/Loire event and the extremal dependence coefficient χ (Figure 4, panel (b)). For the raw climate simulations, H_0 is rejected only for BCC. As detailed in the previous Section, CDF-t does not modify the extremal dependence coefficient χ, but the sequential 2-fold experiment may modify its value. This explains the differences in the χ values between the uncorrected climate simulations and the ones corrected by CDF-t. Despite these limited differences, H_0 is only rejected for BCC corrected by CDF-t. It is never rejected for the multivariate BC methods. However, the medians are more dispersed and the variability intervals are smaller for all climate simulations. The reduction of variability is due to the unique split into training and evaluation subsets, while the spread of the medians is due to the non-stationarity between the two periods.

Regarding RP (Figure 4, panel (d)), as was the case with the random 2-fold experiment, H_0 is rejected for two raw climate simulations (BCC and IPSL) and for 6 of them (out of 10) the medians of the estimated return periods are larger than 10^5 years. Climate simulations are overall well corrected by the three BC methods but quite differently than in the previous experiment: the medians are a bit more dispersed and the variability bars are sometimes smaller than in the random 2-fold experiment, but there are notable exceptions. A striking example is R^2D^2 applied to MRI-ESM2: the median is above 10^3 years, whereas it is close to the ERA5 median in all other cases. On the contrary, when focusing on CDF-t applied to BCC, RP is very well corrected in the sequential experiment, whereas in the random experiment, the median is about 100 times larger than the ERA5

https://doi.org/10.5194/egusphere-2026-3269
Preprint. Discussion started: 19 June 2026

median, albeit not significantly different. This unexpected behavior can partly be explained by a compensation phenomenon between the biased χ and an evolution bias of the margins in the sequential experiment.

A similar analysis can be conducted for the Ahr event (Figure 5, right column). No major changes can be noted for the uncorrected and CDF-t corrected χ values (panel (b)) when compared to the random experiment (panel (a)). For dOTC, the variability is lower for most of the climate simulations, but four of them have medians different from 0 (compared to two in panel (a)). Eight of the ten R^2D^2 corrected simulations have a variability of 0, whereas the two other have medians close to the upper limit of the ERA5 variability interval, although not significantly different. This is due to the unique partitioning of the sequential 2-fold experiment.

When looking at RP (Figure 5, panel (d)), there are several important differences as compared to the random 2-fold experiment: H_0 gets rejected twice, the medians are more dispersed and the variability intervals are often tighter. The spread of the medians is particularly visible for R^2D^2, with H_0 being rejected for CNRM-ESM2 and the median of MIROC6 being at 10^5 years. Again, the reduction of variability is due to the unique separation into training and validation subsets, while the spread of the medians is due to the non-stationarity between the two periods.

According to this experiment, BC methods are relevant tools for providing corrected values for the two considered extremal statistics in a non-stationary context. It comes at the cost of slightly less accurate estimates than in the stationary context and, in some particular cases, R^2D^2 may even degrade the return period. One explanation could be that R^2D^2 modifies the temporal correlation of the variables: this idea will be further explored in Section 5.5.

5.4 The influence of bias correction on climate change signal

Now, BC methods are calibrated on the whole 1992-2021 period and applied to three future periods, as described in Section 4.2. For each of the 10 climate model simulations and each of the four periods, the medians of the coefficients of extremal dependence χ and return periods RP are presented respectively on Figures 6 and 7 for the Seine/Loire event and on Figures 8 and 9 for the Ahr event. Dotted lines represent the 95% variability interval estimated through bootstrap. The red cross to the left represents the ERA5 value estimated on the whole 1992-2021 period. CDF-t corrected values of χ being close to the uncorrected ones, they are not represented.

To assess whether BC methods modify the climate change signal in terms of compound event statistics, this signal must first be determined in the raw climate simulations. According to literature, the climate change signals of extreme precipitation and of extreme accumulated precipitation are not clear: the evolution of these extremes does not follow a monotonous increase or decrease, but often presents some variations (Calvin et al., 2023). For RP, regarding both events, only one of the raw climate simulations (in gray) show a monotonic evolution along all four periods: BCC for the Seine/Loire event is monotonically decreasing (Figure 7). The other climate simulations show either little variations, for example IPSL for the Seine/Loire event (Figure 7) and MIROC6 for the Ahr event (Figure 9), or complex variations, for example CNRM-ESM2 for both events (Figure 7 and 9).

https://doi.org/10.5194/egusphere-2026-3269
Preprint. Discussion started: 19 June 2026

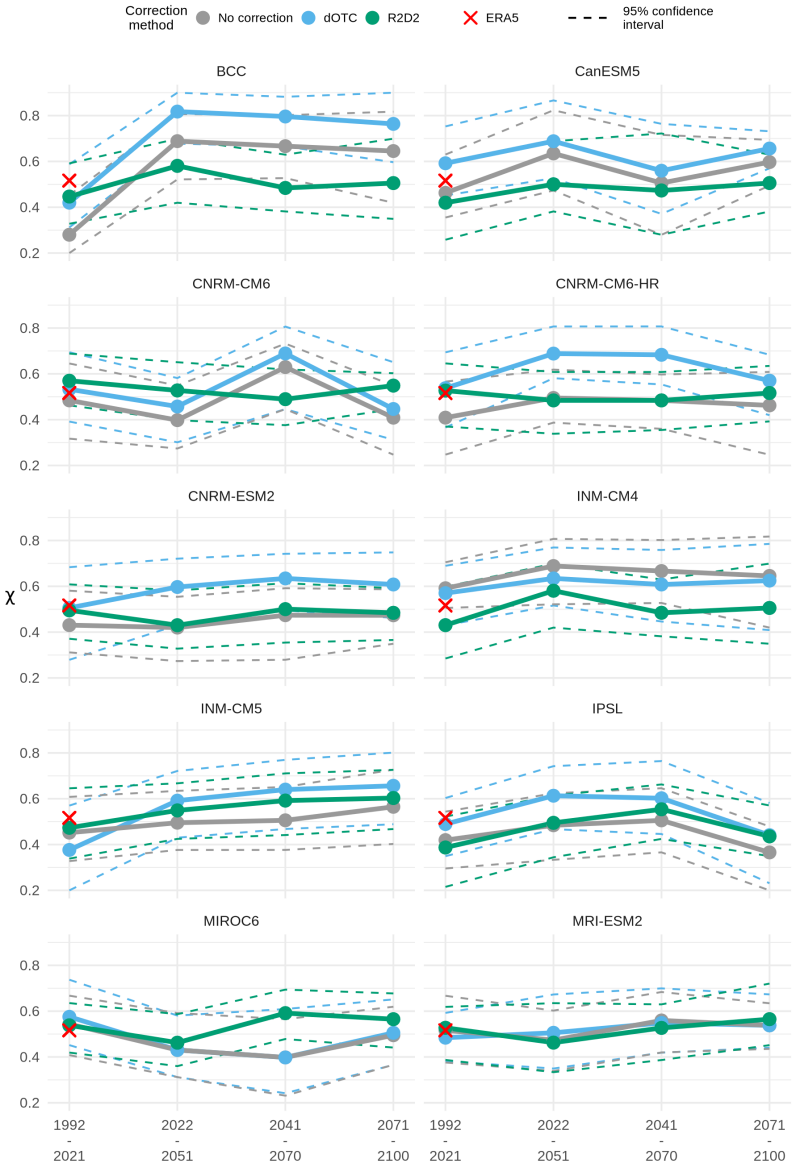

Figure 6. Coefficient of extremal dependence χ for the Seine/Loire event over four 30-year periods, for each of the 10 climate simulations. CDF-t results are not represented as they are similar to the results without correction.

Evolution of χ

To better understand whether the evolutions of the coefficient of extremal dependence χ are kept by the BC methods, Table 2 summarizes the evolution between all pairs of adjacent periods, for every BC method and for both events. Remind that CDF-t

https://doi.org/10.5194/egusphere-2026-3269
Preprint. Discussion started: 19 June 2026

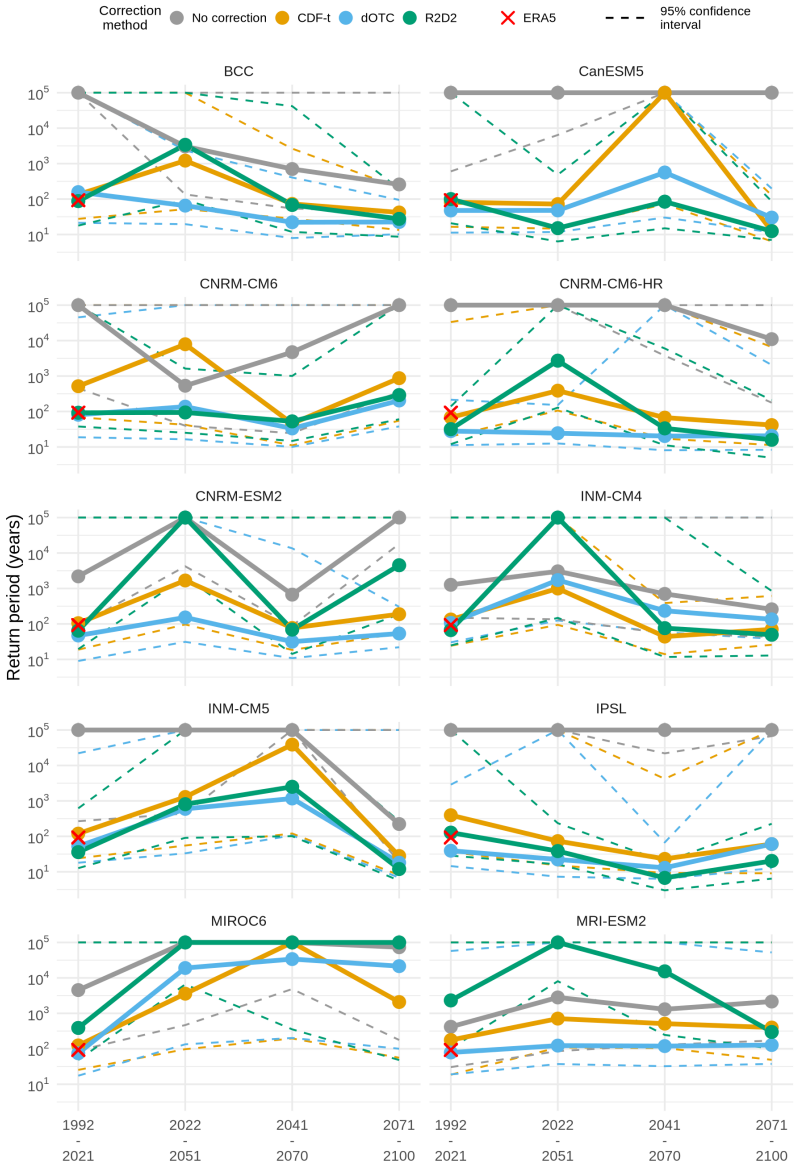

Figure 7. Bivariate return period RP for the Seine/Loire event over four 30-year periods, for each of the 10 climate simulations.

is not represented for χ as the values are similar to the uncorrected ones. First, for each raw climate simulation and each pair of adjacent periods, the evolution of χ is summarized by its trend: increasing if the value of χ increases with the periods, decreasing in the opposite case, and stationary if the values of both periods are equal to 0. There are hence 30 raw trends per event (10 climate simulations and 3 evolutions between adjacent periods). Then, for each BC method, the number and percentage of agreements for the trends are computed. A BC method is said to be in agreement with the raw climate simulation

https://doi.org/10.5194/egusphere-2026-3269
Preprint. Discussion started: 19 June 2026

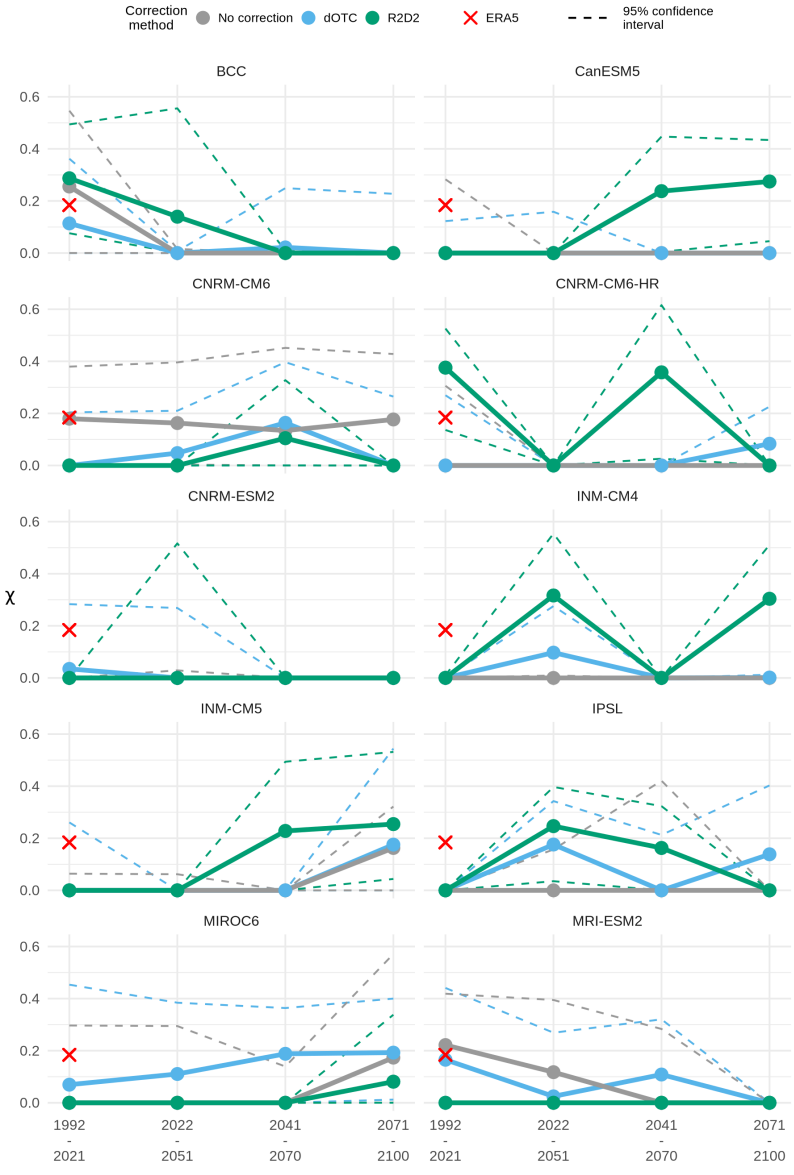

Figure 8. Similar to Fig 6 but for the Ahr event. For the same reason, CDF-t is not represented.

if the corrected χ values present the same trend as the uncorrected ones over the same adjacent periods. In such a case, the BC method is said to preserve the trend of the climate simulation.

In this study, the sign of the trend is not of interest therefore only the stationary trends are separated from the evolutions (increasing or decreasing) in Table 2. It can be noted that χ values corrected by dOTC follow the same evolution as the uncorrected ones most of the time (87%), whereas χ values corrected by R^2D^2 follow it in less cases (67%). The example of

https://doi.org/10.5194/egusphere-2026-3269
Preprint. Discussion started: 19 June 2026

Figure 9. Similar to Fig 7 but for the Ahr event.

CNRM-CM6 for the Seine/Loire event (Figure 6) is quite telling: χ values corrected by dOTC follow the same variations as the uncorrected ones, whereas χ values corrected by R^2D^2 show opposite variations over the last three periods. Remind that for the Ahr event (Figure 8), the ERA5 χ value without bootstrap is equal to 0 and most raw climate simulations have the same value and show stationary evolution (21 over 30, see Table 2). Both multivariate BC methods exhibit some variations and

https://doi.org/10.5194/egusphere-2026-3269
Preprint. Discussion started: 19 June 2026

values different from 0 (only 33% of agreement when stationarity in raw simulations) that can be explained by the sensitivity of the GPD-copula modeling used to represent the Ahr event.

	Seine/Loire		Ahr	
Bias Correction method	**dOTC**	**R²D²**	**dOTC**	**R²D²**
Evolution in raw simulations	**30**		**9**	
Agreement (**number** and %)	**26** (87%)	**20** (67%)	**4** (44%)	**4** (44%)
Stationarity in raw simulations	**0**		**21**	
Agreement (**number** and %)	**0**	**0**	**7** (33%)	**7** (33%)

Table 2. Trend of the evolution of the coefficient of extremal dependence χ between two adjacent periods for the Seine/Loire event and the Ahr event.

Evolution of RP

Table 3 summarizes the trends of the return period RP between two adjacent periods, for every BC method and for both events. The trend is undetermined if the return periods of both periods are censored at 10^5 years.

For the Seine/Loire event and the raw climate simulations, there is an evolution in 19 cases and an indetermination in the other 11 cases (see Table 3). For example, CDF-t is in agreement with the raw climate simulations in 14 out of 19 cases (74%). Overall, the BC methods agree with the raw climate simulations around 75% of the time. With 79%, dOTC seems to be slightly more in agreement with the raw climate simulations than CDF-t (74%) and R²D² (74%). This conclusion has to be qualified by the fact that one third of the cases are undetermined due to raw climate simulations with censored return periods, thereby leading to a reduced sample to determine the preservation of the trend.

	Seine/Loire			Ahr		
Bias Correction method	**CDF-t**	**dOTC**	**R²D²**	**CDF-t**	**dOTC**	**R²D²**
Evolution in raw simulations		**19**			**28**	
Agreement (**number** and %)	**14** (74%)	**15** (79%)	**14** (74%)	**22** (79%)	**19** (68%)	**16** (57%)
Indetermination in raw simulations		**11**			**2**	

Table 3. Trend of the evolution of the return periods between two adjacent periods for the Seine/Loire event and the Ahr event.

Similar consideration can be made for the Ahr event (see Table 3). For raw climate simulations, an evolution is observed in 28 cases, which leaves only 2 undetermined cases. The percentage of agreement is the highest for CDF-t (79%), close to the one for the Seine/Loire event (74%). The percentage is slightly lower for dOTC (68%) but remains high. However, R²D² only agrees with the raw climate simulations in 57% of the cases, which is lower than the two other BC methods and lower than with the Seine/Loire event (74%).

It appears that in around 75% of the cases, the sign of the evolution is correctly preserved. However, this simple summary does not account for all the different behaviors among the climate simulations and the BC methods. Some climate simula-

https://doi.org/10.5194/egusphere-2026-3269
Preprint. Discussion started: 19 June 2026

tions are highlighted to illustrate contrasted behaviors. For the Seine/Loire event (Figure 7), the uncorrected return periods of CanESM5 are censored for all periods, but those of the three BC methods show an increasing trend between 2022-2051 and 2041-2070, followed by a decreasing trend between 2041-2070 and 2071-2100. For IPSL, the return periods of the three BC follow the same evolution whereas the uncorrected ones are censored. In these two cases, event though the agreement between the BC methods and the uncorrected climate simulation cannot be acknowledged, the agreement between the BC methods give confidence in their capacity to capture an overall evolution. In two other cases, there is a lack of agreement between the simulations and the BC methods: CNRM-CM6 for the Seine/Loire event (Figure 7) and MRI-ESM2 for the Ahr event (Figure 9). These four examples emphasize the diversity of behaviors of the BC methods in the context of preserving evolution.

To conclude, BC methods preserve the evolutions of both extremal statistics in most cases. More precisely, for the Seine/Loire event, the evolutions of the uncorrected coefficient of extremal dependence χ are almost always preserved by dOTC and often preserved by R^2D^2. The assumption of the stationarity of the dependence structure by R^2D^2 can explain this difference between the two BC methods. For the Ahr event, the evolution of χ is mostly stationary: both BC methods show difficulties to preserve this stationarity which can be explained by the sensitivity of the GPD-copula modeling. The evolutions of the return period are preserved in around 75% of the cases across both events. R^2D^2 shows slightly less consistency than CDF-t and dOTC, especially for the Ahr event.

5.5 The impact of bias correction on the extremal temporal correlation

Another aspect of the BC methods that can be evaluated is whether and how they modify the temporal correlation of the variables. Some climate variables, such as the API, present strong temporal correlation, which leads the extremes of the variable to occur in groups called "clusters". The temporal correlation of the extremes is taken into account using the extremal index θ, see Leadbetter et al. (1983) for the original definition and Nandagopalan (1994) and Beirlant et al. (2006) for an extension to the bivariate case. The extremal index quantifies the temporal dependence of a process in its extreme values. It belongs to the interval $(0, 1]$, with $\theta = 1$ corresponding to temporal independence. It is usually interpreted as the inverse of the mean cluster size (Moloney et al., 2019). For example, on the ERA5 data, the estimate of the bivariate extremal index of the Seine/Loire event is $\theta = 0.34$ (Jacquemin et al., 2026), which can be interpreted as extremes being clustered in groups of average length equal to $1/0.34 \simeq 3$ days.

The same experiments as those described in Section 4.1 are conducted to compute the joint exceedance probability and the extremal index. These two statistics are linked to the return period RP, see details in Jacquemin et al. (2026). Considering the joint exceedance probability allows us to evaluate the BC methods as was done with the return period RP, but without the impact of the extremal temporal correlation, encapsulated by the extremal index θ. Comparing the extremal index values allows to evaluate whether the BC methods modify the extremal temporal correlation with respect to the reference. The joint exceedance probability is estimated either with the bi-GPD or the GPD-copula modeling (see Section 3.3) and the extremal index θ is estimated using the Dgaps estimator proposed in Holešovskỳ and Fusek (2020). Note that estimated probabilities below 10^{-7} are censored to that value. A statistical test similar to the one in Section 5.2 is performed between the bootstrapped

https://doi.org/10.5194/egusphere-2026-3269
Preprint. Discussion started: 19 June 2026

values for θ and to bring more stability, between the logarithm of the bootstrapped values for the joint exceedance probability. Recall that the null hypothesis is "H_0: the expectations of the two statistics are equal".

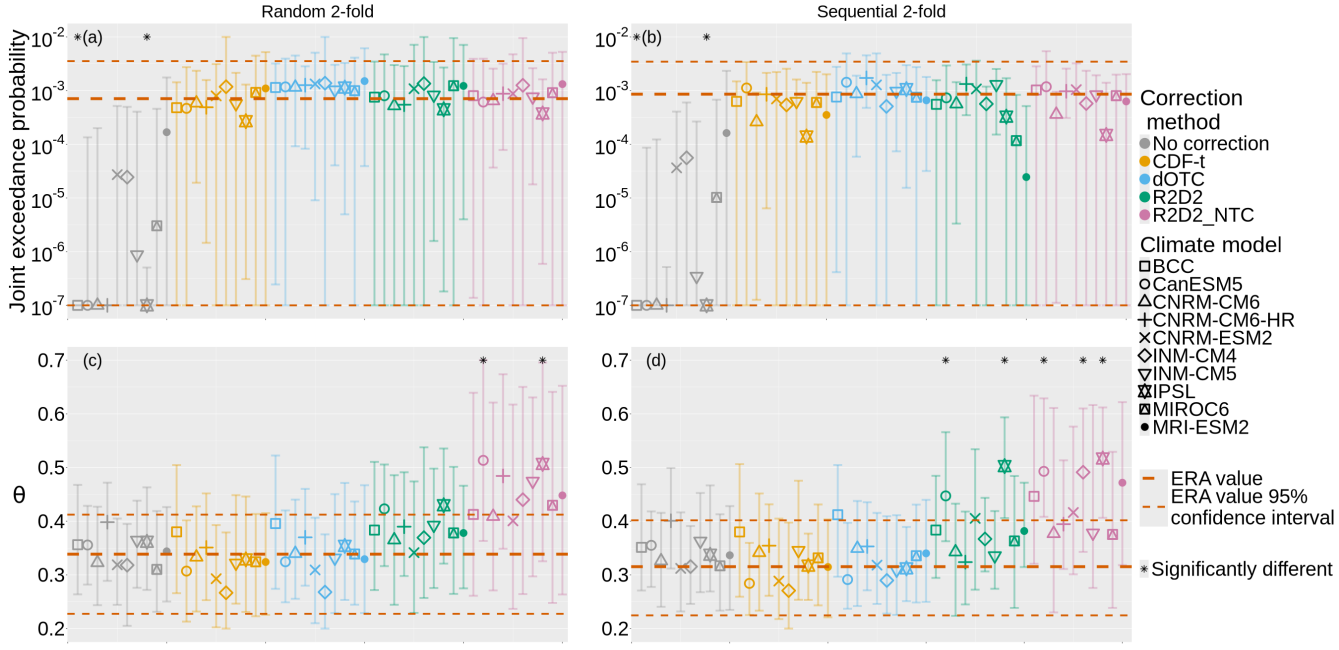

Figure 10. Joint exceedance probability (a, b) and bivariate extremal index θ (c, d) for the Seine/Loire event over the reference period (1992-2021), for the random 2-fold experiment (a, c) and the sequential 2-fold experiment (b, d). See details in Section 4.1.

Seine/Loire event

For the Seine/Loire event, Figure 10 shows the joint exceedance probability and the bivariate extremal index θ in panels (a) and (b) respectively for the random 2-fold experiment and in panels (c) and (d) for the sequential 2-fold experiment over the reference period (1992-2021). Figure 11 is similar but for the Ahr event. The R^2D^2 version with no temporal correlation (named R^2D^2_NTC) mentioned in Section 3.1 is added. On Figure 10 and 11, it is represented in pink, on the right of each panel. One consequence of not taking the temporal correlation into account is that R^2D^2_NTC corrects χ to the exact value of ERA5 for all climate simulations (not shown). Its addition allows to put into perspective the interest of taking into account the temporal correlation by R^2D^2 (Vrac and Thao, 2020).

The joint exceedance probability is incorrectly represented in the raw climate simulations (panels (a) and (b) of Figure 10), with the ERA5 median being outside the variability interval for most of them. H_0 is rejected for only two climate simulations (BCC and IPSL for both experiments), but five median values are censored at 10^{-7} for each experiment. The joint exceedance probability is accurately corrected by all the BC methods. Note that panels (a) and (b) of Figure 10 are similar to panels (c)

https://doi.org/10.5194/egusphere-2026-3269
Preprint. Discussion started: 19 June 2026

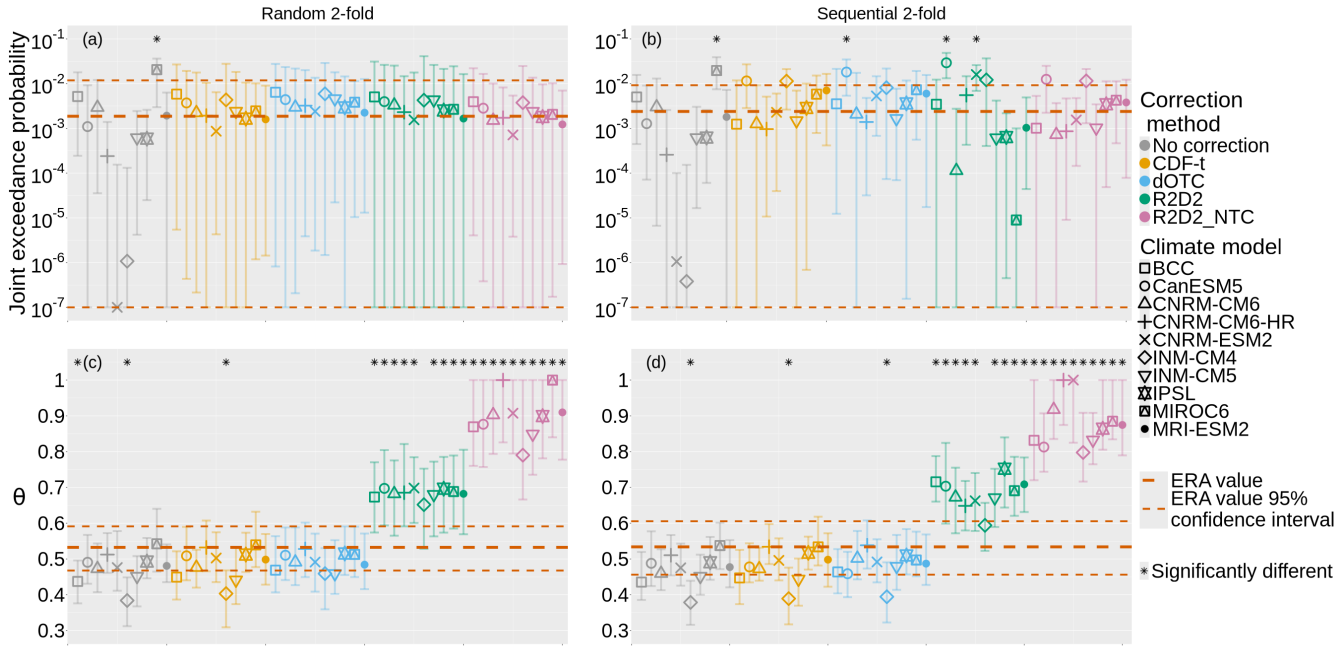

Figure 11. Similar to Figure 10 but for the Ahr event.

and (d) of Figure 4, up to an inverse transformation. This similarity is explained by the accuracy of the estimation of θ both in the raw and in the corrected climate simulations.

Regarding θ, H_0 is not rejected for any of the raw climate simulations on both experiments (panels (c) and (d) of Figure 10). It is also not rejected for any of the climate simulations corrected by CDF-t or dOTC. However, R^2D^2_NTC corrected values are biased: all the medians are close to or above the ERA5 upper interval limit. H_0 is also rejected for two simulations in the random experiment and for three in the sequential experiment. Taking the temporal correlation into account in R^2D^2 allows to reduce this bias as H_0 is not rejected for any simulations corrected by R^2D^2 in the random experiment and is rejected for only two of them in the sequential experiment (CanESM5 and IPSL). Nevertheless, R^2D^2 corrected values are still slightly biased towards higher values, with all the medians above the ERA5 median and two of them above the ERA5 upper interval limit, for both experiments. Note that R^2D^2_NTC accurately corrects the joint exceedance probabilities (panels (a) and (b)) and even seem to outperform R^2D^2 on two simulations with the sequential experiment (MIROC6 and MRI-ESM2, panel (b)). This illustrates that R^2D^2_NTC is relevant to correct the joint exceedance probability when the extremal temporal correlation is not of interest. R^2D^2 can efficiently be constrained in order to limit the degradation of the extremal temporal correlation, but it may comes at the cost of a less precise correction of the joint exceedance probability.

https://doi.org/10.5194/egusphere-2026-3269
Preprint. Discussion started: 19 June 2026

Ahr event

A similar behavior can be observed for the Ahr event in Figure 11. The joint exceedance probability is accurately corrected for most of the climate simulations by the BC methods (panels (a) and (b)). For the extremal index θ (panels (c) and (d)), H_0 is rejected only three times for the raw climate simulations across both experiments. H_0 is rejected twice for CDF-t corrected simulations, and once for dOTC. However, the θ values of simulations corrected with R^2D^2_NTC are strongly biased, close to the upper value $\theta = 1$ corresponding to independence. Similarly to what was observed on the Seine/Loire event, those corrected with R^2D^2 are closer to the ERA5 intervals, but nonetheless still biased. It is probably due to the parameters used to constrain the temporal correlation that can be improved (see Appendix A). For R^2D^2_NTC, the Schaake Shuffle destroys the temporal correlation of the variable that is not the pivot (the precipitation PR), thus leading to θ values close to 1.

The bias towards higher values with R^2D^2_NTC is stronger for the Ahr event than for the Seine/Loire event (panels (c) and (d) of Figures 10 and 11). This could be linked to the choice of the pivot and to the difference of temporal dynamic between the two variables. Recall that the pivot is the API of the Seine for the Seine/Loire event and the precipitation PR for the Ahr event (see Section 3.1). To investigate the influence of the choice of the pivot, the joint exceedance probability and the bivariate extremal index θ are represented on Figure 12 with R^2D^2 and R^2D^2_NTC, and with both variables as the pivot. On both experiments, it clearly appears that the θ values are more biased with the precipitation PR as the pivot (in green and pink) than they are with the API as the pivot (in blue and red), both with R^2D^2 and R^2D^2_NTC (panels (c) and (d)). Note that θ values are slightly biased above the ERA5 upper interval limit for both experiments with R^2D^2_NTC and the API as the pivot, whereas H_0 is only rejected once across both experiments for θ values corrected with R^2D^2 and the API as the pivot. This illustrates that the choice of the pivot can impact the quality of the extremal temporal dependence. The API is by construction a temporally correlated variable, unlike the precipitation: the univariate extremal index of the API is thus lower than that of precipitation, which is close to 1. It seems that selecting the variable with the lowest univariate extremal index value (i.e., the most temporally correlated variable in the extremes) for the pivot (here, the API) limits the degradation of the bivariate extremal temporal correlation.

Figure S1 in Appendix A is similar to Figure 12 but for the Seine/Loire event, with the API of the Seine and the API of the Loire as the pivots. For the θ values (panels (c) and (d)), no strong differences can be observed between the two pivots. Indeed, both variables used for the Seine/Loire event have similar temporal dynamics and similar extremal temporal correlation. For such events, the choice of the pivot does not seem to impact the extremal temporal correlation and moreover, it is less degraded by R^2D^2_NTC than for a CE with variables presenting different dynamics.

To conclude, the extremal temporal correlation of the variables is an important parameter of the compound events under study. Some BC methods may accurately correct the joint exceedance probability but degrade the extremal temporal correlation, which would result in biased return periods. It is thus mandatory to verify that climate simulations accurately reproduce the extremal temporal correlation of the reference variables, and to select a BC method that does not modify it too much. For the two CEs studied here, we can conclude that CDF-t and dOTC do not modify the extremal temporal correlation too much. However, R^2D^2_NTC can strongly degrades it depending on the choice of the pivot. R^2D^2 can be constrained to limit this degradation but

https://doi.org/10.5194/egusphere-2026-3269
Preprint. Discussion started: 19 June 2026

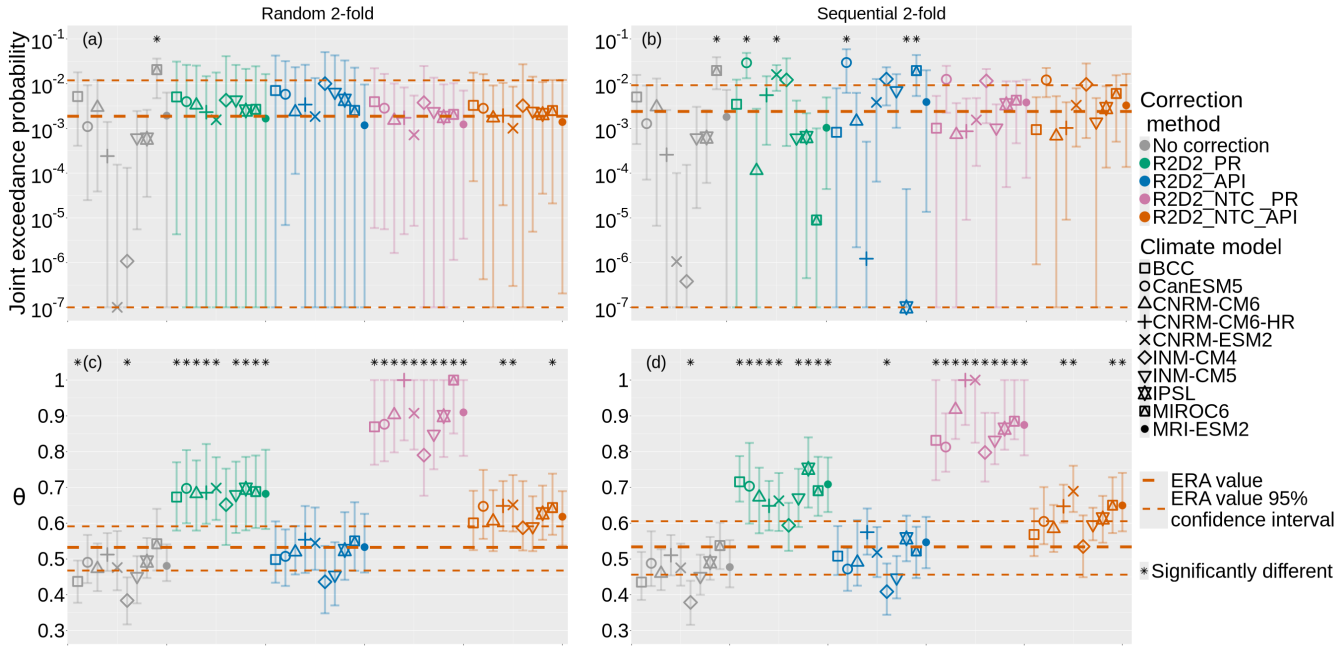

Figure 12. Joint exceedance probability (a, b) and bivariate extremal index θ (c, d) for the Ahr event over the reference period (1992-2021), for the random 2-fold experiment (a, c) and the sequential 2-fold experiment (b, d). See details in Section 4.1. The focus is made on R^2D^2 and R^2D^2_NTC with both the daily precipitation PR and the API as the pivot (see Section 3.1).

the optimization of two parameters is required (Vrac and Thao, 2020). Finally, the variable with the lowest univariate extremal index should be chosen for the pivot as it helps limiting the degradation of the extremal temporal correlation.

6 Conclusion

This work addressed the question of the realism of two extreme rainfall CEs in climate simulations and their improvement with (multivariate) BC methods. The ability of (multivariate) BC methods to preserve the climate change signal of raw climate simulation outputs was also discussed for the two CEs studied here.

Hence, two multivariate BC methods (dOTC and R^2D^2) were compared to a univariate BC method (CDF-t) on their capability to correct two extremal statistics (χ and RP) in the context of two CEs. If the extremal dependence (χ) is well represented in the raw climate simulations, CDF-t appears to be sufficient for both events studied. Otherwise, a multivariate BC method should be used. Both dOTC and R^2D^2 lead to an improved estimation of χ and of the return period RP over the calibration period, in a stationary and in a non-stationary context. However, careful selection of the pivot and optimization of R^2D^2 are necessary in order to minimize the modification of the extremal temporal correlation. The variable with the lowest univariate

https://doi.org/10.5194/egusphere-2026-3269
Preprint. Discussion started: 19 June 2026

extremal index should be chosen for the pivot and the optimization of the R^2D^2 parameters can be achieved by considering the statistics of interest within some 2-fold experiments similar to the ones presented here.

Their ability to preserve the climate change signal was also investigated. All tested BC methods seem to preserve the temporal evolution of the return period in around 75% of the cases. Only R^2D^2 showed some limitations in preserving the evolution of the raw climate simulations, both in terms of return period RP and coefficient of extremal dependence χ. This behavior was expected as, by construction, R^2D^2 assumes the stationarity of the dependence structure. It is important to note that the climate change signal for extremes of precipitation and of API is complex, non-monotonic, and that the climate simulations used in this article do not agree between themselves. For practitioners, we advise to assess the ability of the chosen BC method to preserve the evolution of the climate simulation on each case study.

To conclude, this study showed that multivariate bias correction methods improve the realism of extreme rainfall compound events and that, in most cases, they preserve their evolution under climate change.

A first perspective for this study would be to spatially extend the analysis of the two CEs. Other watersheds could be considered as spatially compound events. For preconditioned compound events, a similar analysis could be conducted for all grid cells in Europe. However, the conclusions of this study could differ when studying similar events at other locations or with other types of CEs. A second perspective would be to apply the framework proposed in this article to other CEs, such as compound hot and dry events, false springs or winter storms. This analytical framework is theoretically general enough to assess the evolution of such compound events but technical limitations may arise. Moreover, this study was limited to bivariate CEs: statistical frameworks and multivariate BC methods can be extended to more than two dimensions but the conclusions may differ.

Also, it is important to note that the two multivariate bias correction methods tested in this work (dOTC and R^2D^2) are designed to correct the whole distribution and not specifically the extremes. Therefore, another line of research would be to design a multivariate bias correction method which would focus on extreme values. This could improve the way extreme events are represented in the climate simulations and therefore provide a more accurate insight about their temporal evolutions. Some attempts have been made (Byun and Hamlet, 2024; Holthuijzen et al., 2022) but they lack the theoretical background to ensure an effective correction of extremes and extremal dependence.

Another related field that may be relevant to this study is that of attribution. Indeed, attribution of extreme events quantifies the degree to which climate change has altered the probability or intensity of a specific extreme event (Stott et al., 2004). This quantification is realized through counterfactual simulations: a world with anthropogenic forcing is compared to one without. As stated in Philip et al. (2020), bias correction methods are not always used in attribution studies. Moreover, when an attribution study correct the biases of the simulations, it is usually done with an additive or a multiplicative correction, which may not be adapted for the extremes (Philip et al., 2020). Hence, the bias correction methods studied here (CDF-t, dOTC and R^2D^2) could be used in the context of attributing compound events (Zscheischler and Lehner, 2022), to better characterize them both in the factual and counterfactual worlds (Jeon et al., 2016; Wang et al., 2025). These bias correction methods could lead to a better estimation of the probability of occurrence of compound events and to a better quantification of the influence of climate change on their evolution.

https://doi.org/10.5194/egusphere-2026-3269
Preprint. Discussion started: 19 June 2026

Data availability. The CMIP6 model simulations can be downloaded through the Earth System Grid Federation portals. Instructions to access the data are available here: https://pcmdi.llnl.gov/mips/cmip6/data-access-getting-started.html. The ERA5 reanalysis data used as reference in this study can be accessed via the "Climate Data Store" (CDS) web portal https://cds.climate.copernicus.eu.

Appendix A: Technical details

The packages and parameters used to get the described results are detailed in this technical Appendix. Data are presented in section 2.1.

Technical details for the computation of the bias correction

Bias correction is done in Python (version 3.13.9) using the SBCK package (version 2.0.0a46). The Statistical Bias Correction Kit (SBCK) is developed by Yohan Robin and can be found here https://github.com/yrobink/SBCK-python/tree/version-2.X.Y. Following the protocol of section 4.1, the data is separated (randomly or sequentially), BC methods are learned and applied, then the corrected datasets are merged and saved. Some PrePostProcessing (PPP) methods are used, namely the "LFLoglin" and the "FilterWarnings" ones. The "LFLoglin" method applies a log-linear function to the data before the bias correction, and the inverse transform after the BC. It ensures the positivity of the values after BC. For the Ahr event, the "SSR" method is also used for CDF-t and R^{2}D^2. The "SSR" method transforms values equal to 0 into random values between 0 and the smallest strictly positive value. The BC method is applied and the data below a threshold (given or inferred from the reference data) are transformed back into 0.

The specific parameters for CDF-t are $norm = origin$ and $oob = Y0$. For dOTC, a bin width of $[0.25, 0.25]$ is specified. R^{2}D^2 requires a univariate BC method: CDF-t is used for the different versions of R^{2}D^2. For R^{2}D^2_NTC, the pivot is a single variable (discussed in section 3.1 and the same parameters as CDF-t are used. Finally, similar parameters are used for R^{2}D^2, and the parameters lag_search and lag_keep are set at 6 and 3 respectively, the default proposed values.

Technical details for the computation of the statistics

The bootstrap and the computation of the statistics are done in R (version 4.3.1). The package bi-GPD developed by Grégoire Jacquemin is used (see Jacquemin et al. (2026) for more details and https://github.com/gjacqueminFR/biGPD for the code). The mev package (Belzile [aut et al., 2024) is modified to accept $\xi > -0.5$ and used to estimate the parameters of the EGPD. The EGPD of type 4 is used, with the estimation function initialized at $(0.5, 1.5, 4.5, 6, -0.05)$ for the Seine variable and at $(0.5, 0.9, 4.5, 8, -0.05)$ for the Loire variable. As detailed in section 5.5, the bivariate extremal index θ is estimated over the complete data, and its value is used for the bootstrapped iteration. The Dgaps package (Holešovskỳ and Fusek, 2020) is used to estimate the value of θ, with $Dparam = 3$.

For the GPD-copula modeling, most of the technical details are given in section 3.2. It can be mentioned that if less than four unique values for any of the two variables should be used to select the copula family, then the independent copula is chosen instead. Code is available upon demand to the corresponding author.

https://doi.org/10.5194/egusphere-2026-3269
Preprint. Discussion started: 19 June 2026

Author contributions. All authors designed the experiments and GJ carried them out. GJ developed the model code and performed the simulations. GJ prepared the manuscript with contributions from all co-authors.

Competing interests. The authors declare that they have no conflict of interest.

Acknowledgements. We thank the Copernicus Climate Change Services for making the ERA5 reanalyses available. This work has been supported by the chair Geolearning, funded by ANDRA, BNP Paribas, CCR and the SCOR Foundation for Science. We also acknowledge the support of the COESION project funded by the French National program LEFE (Les Enveloppes Fluides et l'Environnement). This work also benefited from state aid managed by the National Research Agency under France 2030 bearing the references ANR-22-EXTR-0005 (TRACCS-PC4-EXTENDING project).

https://doi.org/10.5194/egusphere-2026-3269
Preprint. Discussion started: 19 June 2026

References

Adeyeri, O., Laux, P., Lawin, A., and Oyekan, K.: Multiple bias-correction of dynamically downscaled CMIP5 climate models temperature projection: a case study of the transboundary Komadugu-Yobe river basin, Lake Chad region, West Africa, SN Applied Sciences, 2, 1221, https://doi.org/https://doi.org/10.1007/s42452-020-3009-4, 2020.

Allard, D., Vrac, M., François, B., and García de Cortázar-Atauri, I.: Assessing multivariate bias corrections of climate simulations on various impact models under climate change, Hydrology and Earth System Sciences, 29, 4711–4738, https://doi.org/10.5194/hess-29-4711-2025, 2025.

Beirlant, J., Goegebeur, Y., Segers, J., and Teugels, J. L.: Statistics of extremes: theory and applications, John Wiley & Sons, https://doi.org/10.1002/0470012382, 2006.

Belzile [aut, L., cre, Wadsworth, J. L., Northrop, P. J., Grimshaw, S. D., Zhang, J., Stephens, M. A., Owen, A. B., and Huser, R.: mev: Modelling of Extreme Values, https://cran.r-project.org/web/packages/mev/index.html, 2024.

Bevacqua, E., Maraun, D., Hobæk Haff, I., Widmann, M., and Vrac, M.: Multivariate statistical modelling of compound events via pair-copula constructions: analysis of floods in Ravenna (Italy), Hydrology and Earth System Sciences, 21, 2701–2723, https://doi.org/10.5194/hess-21-2701-2017, 2017.

Blanchard, B. J., McFarland, M. J., Schmugge, T. J., and Rhoades, E.: ESTIMATION OF SOIL MOISTURE WITH API ALGORITHMS AND MICROWAVE EMISSION, JAWRA Journal of the American Water Resources Association, 17, 767–774, https://doi.org/10.1111/j.1752-1688.1981.tb01296.x, 1981.

Boucher, O., Denvil, S., Levavasseur, G., Cozic, A., Caubel, A., Foujols, M.-A., Meurdesoif, Y., Cadule, P., Devilliers, M., Ghattas, J., Lebas, N., Lurton, T., Mellul, L., Musat, I., Mignot, J., and Cheruy, F.: IPSL IPSL-CM6A-LR model output prepared for CMIP6 CMIP, https://doi.org/10.22033/ESGF/CMIP6.1534, 2018.

Brett, L., White, C. J., Domeisen, D. I. V., van den Hurk, B., Ward, P., and Zscheischler, J.: Review article: The growth in compound weather and climate event research in the decade since SREX, Natural Hazards and Earth System Sciences, 25, 2591–2611, https://doi.org/10.5194/nhess-25-2591-2025, 2025.

Byun, K. and Hamlet, A. F.: An improved empirical quantile mapping approach for bias correction of extreme values in climate model simulations, Environmental Research Letters, 20, 014 041, https://doi.org/10.1088/1748-9326/ad9b3d, 2024.

Bárdossy, A. and Pegram, G.: Multiscale spatial recorrelation of RCM precipitation to produce unbiased climate change scenarios over large areas and small, Water Resources Research, 48, https://doi.org/https://doi.org/10.1029/2011WR011524, 2012.

Calvin, K., Dasgupta, D., Krinner, G., Mukherji, A., Thorne, P. W., Trisos, C., Romero, J., Aldunce, P., Barrett, K., Blanco, G., Cheung, W. W., Connors, S., Denton, F., Diongue-Niang, A., Dodman, D., Garschagen, M., Geden, O., Hayward, B., Jones, C., Jotzo, F., Krug, T., Lasco, R., Lee, Y.-Y., Masson-Delmotte, V., Meinshausen, M., Mintenbeck, K., Mokssit, A., Otto, F. E., Pathak, M., Pirani, A., Poloczanska, E., Pörtner, H.-O., Revi, A., Roberts, D. C., Roy, J., Ruane, A. C., Skea, J., Shukla, P. R., Slade, R., Slangen, A., Sokona, Y., Sörensson, A. A., Tignor, M., Van Vuuren, D., Wei, Y.-M., Winkler, H., Zhai, P., Zommers, Z., Hourcade, J.-C., Johnson, F. X., Pachauri, S., Simpson, N. P., Singh, C., Thomas, A., Totin, E., Arias, P., Bustamante, M., Elgizouli, I., Flato, G., Howden, M., Méndez-Vallejo, C., Pereira, J. J., Pichs-Madruga, R., Rose, S. K., Saheb, Y., Sánchez Rodríguez, R., Ürge Vorsatz, D., Xiao, C., Yassaa, N., Alegría, A., Armour, K., Bednar-Friedl, B., Blok, K., Cissé, G., Dentener, F., Eriksen, S., Fischer, E., Garner, G., Guivarch, C., Haasnoot, M., Hansen, G., Hauser, M., Hawkins, E., Hermans, T., Kopp, R., Leprince-Ringuet, N., Lewis, J., Ley, D., Ludden, C., Niamir, L., Nicholls, Z., Some, S., Szopa, S., Trewin, B., Van Der Wijst, K.-I., Winter, G., Witting, M., Birt, A., Ha, M., Romero, J., Kim, J., Haites, E. F., Jung, Y., Stavins, R.,

https://doi.org/10.5194/egusphere-2026-3269
Preprint. Discussion started: 19 June 2026

Birt, A., Ha, M., Orendain, D. J. A., Ignon, L., Park, S., Park, Y., Reisinger, A., Cammaramo, D., Fischlin, A., Fuglestvedt, J. S., Hansen, G., Ludden, C., Masson-Delmotte, V., Matthews, J. R., Mintenbeck, K., Pirani, A., Poloczanska, E., Leprince-Ringuet, N., and Péan, C.: IPCC, 2023: Climate Change 2023: Synthesis Report. Contribution of Working Groups I, II and III to the Sixth Assessment Report of the Intergovernmental Panel on Climate Change [Core Writing Team, H. Lee and J. Romero (eds.)]. IPCC, Geneva, Switzerland., Tech. rep., Intergovernmental Panel on Climate Change (IPCC), https://doi.org/10.59327/IPCC/AR6-9789291691647, edition: First, 2023.

Cannon, A. J.: Multivariate quantile mapping bias correction: an N-dimensional probability density function transform for climate model simulations of multiple variables, Climate dynamics, 50, 31–49, https://doi.org/https://doi.org/10.1007/s00382-017-3580-6, 2018.

Christensen, J. H., Boberg, F., Christensen, O. B., and Lucas-Picher, P.: On the need for bias correction of regional climate change projections of temperature and precipitation, Geophysical Research Letters, 35, L20 709, https://doi.org/10.1029/2008GL035694, 2008.

Clark, M., Gangopadhyay, S., Hay, L., Rajagopalan, B., and Wilby, R.: The Schaake Shuffle: A Method for Reconstructing Space–Time Variability in Forecasted Precipitation and Temperature Fields, Journal of Hydrometeorology, 5, 243 – 262, https://doi.org/10.1175/1525-7541(2004)005<0243:TSSAMF>2.0.CO;2, 2004.

Coles, S., Heffernan, J., and Tawn, J.: Dependence measures for extreme value analyses, Extremes, 2, 339–365, https://doi.org/10.1023/A:1009963131610, 1999.

De Moraes, M. A. E., Mendes Filho, W. M., and others: Antecedent Precipitation Index to Estimate Soil Moisture and Correlate as a Triggering Process in the Occurrence of Landslides, International Journal of Geosciences, 15, 70–86, https://doi.org/10.4236/ijg.2024.151006, 2024.

Dieng, D., Cannon, A. J., Laux, P., Hald, C., Adeyeri, O., Rahimi, J., Srivastava, A. K., Mbaye, M. L., and Kunstmann, H.: Multivariate Bias-Correction of High-Resolution Regional Climate Change Simulations for West Africa: Performance and Climate Change Implications, Journal of Geophysical Research: Atmospheres, 127, e2021JD034 836, https://doi.org/https://doi.org/10.1029/2021JD034836, 2022.

Déqué, M.: Frequency of precipitation and temperature extremes over France in an anthropogenic scenario: Model results and statistical correction according to observed values, Global and Planetary Change, 57, 16–26, 2007.

El Hachem, A., Seidel, J., and Bárdossy, A.: Probabilistic downscaling of EURO-CORDEX precipitation data for the assessment of future areal precipitation extremes for hourly to daily durations, Hydrology and Earth System Sciences, 29, 1335–1357, https://doi.org/10.5194/hess-29-1335-2025, 2025.

Famien, A. M., Janicot, S., Ochou, A. D., Vrac, M., Defrance, D., Sultan, B., and Noël, T.: A bias-corrected CMIP5 dataset for Africa using the CDF-t method – a contribution to agricultural impact studies, Earth System Dynamics, 9, 313–338, https://doi.org/10.5194/esd-9-313-2018, 2018.

François, B. and Vrac, M.: Time of emergence of compound events: contribution of univariate and dependence properties, Natural Hazards and Earth System Sciences, 23, 21–44, 2023.

François, B., Vrac, M., Cannon, A. J., Robin, Y., and Allard, D.: Multivariate bias corrections of climate simulations: which benefits for which losses?, Earth System Dynamics, 11, 537–562, https://doi.org/10.5194/esd-11-537-2020, 2020.

Gleick, P. H.: Methods for evaluating the regional hydrologic impacts of global climatic changes, Journal of Hydrology, 88, 97–116, https://doi.org/https://doi.org/10.1016/0022-1694(86)90199-X, 1986.

Gumbel, E. J.: The Return Period of Flood Flows, The Annals of Mathematical Statistics, 12, 163–190, https://www.jstor.org/stable/2235766, 1941.

https://doi.org/10.5194/egusphere-2026-3269
Preprint. Discussion started: 19 June 2026

Guo, L., Jiang, Z., Chen, D., Le Treut, H., and Li, L.: Projected precipitation changes over China for global warming levels at 1.5° C and 2° C in an ensemble of regional climate simulations: impact of bias correction methods, Climatic Change, 162, 623–643, https://doi.org/10.1007/s10584-020-02841-z, 2020.

Haddad, Z. S. and Rosenfeld, D.: Optimality of empirical Z-R relations, Quarterly Journal of the Royal Meteorological Society, 123, 1283–1293, https://doi.org/10.1002/qj.49712354107, 1997.

Hay, L. E., Wilby, R. L., and Leavesley, G. H.: A COMPARISON OF DELTA CHANGE AND DOWNSCALED GCM SCENARIOS FOR THREE MOUNTAINOUS BASINS IN THE UNITED STATES, JAWRA Journal of the American Water Resources Association, 36, 387–397, https://doi.org/https://doi.org/10.1111/j.1752-1688.2000.tb04276.x, 2000.

Heinrich, P., Hagemann, S., Weisse, R., and Gaslikova, L.: Changes in compound flood event frequency in northern and central Europe under climate change, Frontiers in Climate, 5, 1227 613, 2023.

Hersbach, H., Bell, B., Berrisford, P., Hirahara, S., and others: The ERA5 global reanalysis, Quarterly Journal of the Royal Meteorological Society, 146, 1999–2049, https://doi.org/10.1002/qj.3803, 2020.

Holešovskỳ, J. and Fusek, M.: Estimation of the extremal index using censored distributions, Extremes, 23, 197–213, https://doi.org/10.1007/s10687-020-00374-3, 2020.

Holthuijzen, M., Beckage, B., Clemins, P. J., Higdon, D., and Winter, J. M.: Robust bias-correction of precipitation extremes using a novel hybrid empirical quantile-mapping method, Theoretical and Applied Climatology, 149, 863–882, https://doi.org/10.1007/s00704-022-04035-2, 2022.

Jacquemin, G., Allard, D., Freulon, X., and Vrac, M.: Return Period of Nonconcurrent Climate Compound Events: A Nonparametric Bivariate Generalized Pareto Approach, Environmetrics, 37, e70 063, https://onlinelibrary.wiley.com/doi/abs/10.1002/env.70063, 2026.

Jeon, S., Paciorek, C. J., and Wehner, M. F.: Quantile-based bias correction and uncertainty quantification of extreme event attribution statements, Weather and Climate Extremes, 12, 24–32, https://doi.org/10.1016/j.wace.2016.02.001, 2016.

Joe, H.: Parametric Families of Multivariate Distributions with Given Margins, Journal of Multivariate Analysis, 46, 262–282, https://doi.org/10.1006/jmva.1993.1061, 1993.

Kass, R. E. and Raftery, A. E.: Bayes factors, Journal of the american statistical association, 90, 773–795, https://doi.org/10.1080/01621459.1995.10476572, 1995.

Kharin, V. V., Flato, G. M., Zhang, X., Gillett, N. P., Zwiers, F., and Anderson, K. J.: Risks from Climate Extremes Change Differently from 1.5°C to 2.0°C Depending on Rarity, Earth's Future, 6, 704–715, https://doi.org/10.1002/2018EF000813, 2018.

Kim, Y., Evans, J. P., and Sharma, A.: Correcting biases in regional climate model boundary variables for improved simulation of high-impact compound events, Iscience, 26, https://doi.org/10.1016/j.isci.2023.107696, 2023a.

Kim, Y., Evans, J. P., and Sharma, A.: Multivariate bias correction of regional climate model boundary conditions, Climate Dynamics, 61, 3253–3269, https://doi.org/10.1007/s00382-023-06718-6, 2023b.

Kohler, M. A. and Linsley, R. K.: Predicting the runoff from storm rainfall, vol. 30, US Department of Commerce, Weather Bureau, 1951.

Leadbetter, M. R., Lindgren, G., and Rootzén, H.: Extremes and related properties of random sequences and processes, Springer Science & Business Media, https://doi.org/10.1007/978-1-4612-5449-2, 1983.

Legrand, J., Ailliot, P., Naveau, P., and Raillard, N.: Joint stochastic simulation of extreme coastal and offshore significant wave heights, The Annals of Applied Statistics, 17, 3363–3383, https://doi.org/10.1214/23-AOAS1766, 2023.

Lemus-Canovas, M. and Lopez-Bustins, J. A.: Assessing internal changes in the future structure of dry–hot compound events: the case of the Pyrenees, Natural Hazards and Earth System Sciences, 21, 1721–1738, https://doi.org/10.5194/nhess-21-1721-2021, 2021.

https://doi.org/10.5194/egusphere-2026-3269
Preprint. Discussion started: 19 June 2026

Li, C., Zwiers, F., Zhang, X., and Li, G.: How Much Information Is Required to Well Constrain Local Estimates of Future Precipitation Extremes?, Earth's Future, 7, 11–24, https://doi.org/10.1029/2018EF001001, 2019.

Li, X., Wei, Y., and Li, F.: Optimality of antecedent precipitation index and its application, Journal of Hydrology, 595, 126 027, https://doi.org/10.1016/j.jhydrol.2021.126027, 2021.

Maraun, D., Wetterhall, F., Ireson, A. M., Chandler, R. E., Kendon, E. J., Widmann, M., Brienen, S., Rust, H. W., Sauter, T., Themeßl, M., Venema, V. K. C., Chun, K. P., Goodess, C. M., Jones, R. G., Onof, C., Vrac, M., and Thiele-Eich, I.: Precipitation downscaling under climate change: Recent developments to bridge the gap between dynamical models and the end user, Reviews of Geophysics, 48, https://doi.org/https://doi.org/10.1029/2009RG000314, 2010.

Mehrotra, R. and Sharma, A.: Correcting for systematic biases in multiple raw GCM variables across a range of timescales, Journal of Hydrology, 520, 214–223, https://doi.org/https://doi.org/10.1016/j.jhydrol.2014.11.037, 2015.

Mehrotra, R. and Sharma, A.: A multivariate quantile-matching bias correction approach with auto-and cross-dependence across multiple time scales: Implications for downscaling, Journal of Climate, 29, 3519–3539, https://doi.org/10.1175/JCLI-D-15-0356.1, 2016.

Mehrotra, R. and Sharma, A.: A Resampling Approach for Correcting Systematic Spatiotemporal Biases for Multiple Variables in a Changing Climate, Water Resources Research, 55, 754–770, https://doi.org/https://doi.org/10.1029/2018WR023270, 2019.

Meng, Y., Hao, Z., Feng, S., Guo, Q., and Zhang, Y.: Multivariate bias corrections of CMIP6 model simulations of compound dry and hot events across China, Environmental Research Letters, 17, 104 005, https://doi.org/10.1088/1748-9326/ac8e86, 2022.

Michelangeli, P.-A., Vrac, M., and Loukos, H.: Probabilistic downscaling approaches: Application to wind cumulative distribution functions, Geophysical Research Letters, 36, https://doi.org/10.1029/2009GL038401, 2009.

Mohr, S., Ehret, U., Kunz, M., Ludwig, P., and others: A multi-disciplinary analysis of the exceptional flood event of July 2021 in central Europe – Part 1: Event description and analysis, Natural Hazards and Earth System Sciences, 23, 525–551, https://doi.org/10.5194/nhess-23-525-2023, 2023.

Moloney, N. R., Faranda, D., and Sato, Y.: An overview of the extremal index, Chaos: An Interdisciplinary Journal of Nonlinear Science, 29, 022 101, https://doi.org/10.1063/1.5079656, 2019.

Nagler, T., Schepsmeier, U., Stoeber, J., Brechmann, E. C., Graeler, B., Erhardt, T., Almeida, C., Min, A., Czado, C., Hofmann, M., Killiches, M., Joe, H., and Vatter, T.: VineCopula: Statistical Inference of Vine Copulas, https://cran.r-project.org/web/packages/VineCopula/index.html, 2025.

Nandagopalan, S.: On the multivariate extremal index, Journal of research of the National Institute of Standards and Technology, 99, 543, https://doi.org/10.6028/jres.099.052, 1994.

Naveau, P., Huser, R., Ribereau, P., and Hannart, A.: Modeling jointly low, moderate, and heavy rainfall intensities without a threshold selection, Water Resources Research, 52, 2753–2769, https://doi.org/10.1002/2015WR018552, 2016.

Olschewski, P., Dieng, M. D. B., Moutahir, H., Böker, B., Haas, E., Kunstmann, H., and Laux, P.: Amplified potential for vegetation stress under climate-change-induced intensifying compound extreme events in the Greater Mediterranean Region, Natural Hazards and Earth System Sciences, 24, 1099–1134, https://doi.org/10.5194/nhess-24-1099-2024, 2024.

O'Neill, B. C., Tebaldi, C., van Vuuren, D. P., Eyring, V., Friedlingstein, P., Hurtt, G., Knutti, R., Kriegler, E., Lamarque, J.-F., Lowe, J., Meehl, G. A., Moss, R., Riahi, K., and Sanderson, B. M.: The Scenario Model Intercomparison Project (ScenarioMIP) for CMIP6, Geoscientific Model Development, 9, 3461–3482, https://doi.org/10.5194/gmd-9-3461-2016, 2016.

Ossberger, J.: tea: Threshold Estimation Approaches, https://cran.r-project.org/web/packages/tea/index.html, 2020.

Panofsky, H. and Brier, G.: Some applications of statistics to meteorology, Penn, State Univ., University Park, Pa, 1958.

https://doi.org/10.5194/egusphere-2026-3269
Preprint. Discussion started: 19 June 2026

Pegram, G. and Bárdossy, A.: Downscaling Regional Circulation Model rainfall to gauge sites using recorrelation and circulation pattern dependent quantile–quantile transforms for quantifying climate change, Journal of Hydrology, 504, 142–159, https://doi.org/https://doi.org/10.1016/j.jhydrol.2013.09.014, 2013.

Philip, S., Kew, S. F., Jan van Oldenborgh, G., Aalbers, E., Vautard, R., Otto, F., Haustein, K., Habets, F., and Singh, R.: Validation of a rapid attribution of the May/June 2016 flood-inducing precipitation in France to climate change, Journal of Hydrometeorology, 19, 1881–1898, https://doi.org/10.1175/JHM-D-18-0074.1, 2018.

Philip, S., Kew, S., van Oldenborgh, G. J., Otto, F., Vautard, R., van der Wiel, K., King, A., Lott, F., Arrighi, J., Singh, R., and van Aalst, M.: A protocol for probabilistic extreme event attribution analyses, Advances in Statistical Climatology, Meteorology and Oceanography, 6, 177–203, https://doi.org/10.5194/ascmo-6-177-2020, 2020.

Pierce, D. W., Cayan, D. R., Maurer, E. P., Abatzoglou, J. T., and Hegewisch, K. C.: Improved Bias Correction Techniques for Hydrological Simulations of Climate Change, Journal of Hydrometeorology, 16, 2421 – 2442, https://doi.org/10.1175/JHM-D-14-0236.1, 2015.

Raäisaänen, J.: How reliable are climate models?, Tellus A: Dynamic Meteorology and Oceanography, 59, 2–29, 2007.

Ridder, N., Ukkola, A., Pitman, A., and Perkins-Kirkpatrick, S.: Increased occurrence of high impact compound events under climate change, Npj Climate and Atmospheric Science, 5, 3, https://doi.org/10.1038/s41612-021-00224-4, 2022.

Robin, Y., Vrac, M., Naveau, P., and Yiou, P.: Multivariate stochastic bias corrections with optimal transport, Hydrology and Earth System Sciences, 23, 773–786, https://doi.org/10.5194/hess-23-773-2019, 2019.

Rootzén, H. and Tajvidi, N.: Multivariate generalized Pareto distributions, Bernoulli, 12, 917 – 930, https://doi.org/10.3150/bj/1161614952, 2006.

Rootzén, H., Segers, J., and Wadsworth, J. L.: Multivariate generalized Pareto distributions: Parametrizations, representations, and properties, Journal of Multivariate Analysis, 165, 117–131, https://doi.org/10.1016/j.jmva.2017.12.003, 2018.

Schröter, K., Kunz, M., Elmer, F., Mühr, B., and Merz, B.: What made the June 2013 flood in Germany an exceptional event? A hydrometeorological evaluation, Hydrology and Earth System Sciences, 19, 309–327, https://doi.org/10.5194/hess-19-309-2015, 2015.

Seferian, R.: IPCC DDC: CNRM-CERFACS CNRM-ESM2-1 model output prepared for CMIP6 CMIP, https://doi.org/10.26050/WDCC/AR6.C6CMCECE1, 2023.

Seneviratne, S., Donat, M., Pitman, A., Knutti, R., and Wilby, R.: Allowable CO2 emissions based on regional and impact-related climate targets, Nature, 529, 477–483, https://doi.org/10.1038/nature16542, 2016.

Shiogama, H., Abe, M., and Tatebe, H.: MIROC MIROC6 model output prepared for CMIP6 ScenarioMIP, https://doi.org/10.22033/ESGF/CMIP6.898, 2019.

Sklar, M.: Fonctions de répartition à n dimensions et leurs marges, Annales de l'ISUP, 8, 229–231, https://hal.science/hal-04094463, 1959.

Stott, P. A., Stone, D. A., and Allen, M. R.: Human contribution to the European heatwave of 2003, Nature, 432, 610–614, https://doi.org/10.1038/nature03089, 2004.

Swart, N. C., Cole, J. N., Kharin, V. V., Lazare, M., Scinocca, J. F., Gillett, N. P., Anstey, J., Arora, V., Christian, J. R., Jiao, Y., Lee, W. G., Majaess, F., Saenko, O. A., Seiler, C., Seinen, C., Shao, A., Solheim, L., von Salzen, K., Yang, D., Winter, B., and Sigmond, M.: CCCma CanESM5 model output prepared for CMIP6 ScenarioMIP, https://doi.org/10.22033/ESGF/CMIP6.1317, 2019.

Teng, W., Wang, J., and Doraiswamy, P.: Relationship between satellite microwave radiometric data, antecedent precipitation index, and regional soil moisture, International Journal of Remote Sensing, 14, 2483–2500, https://doi.org/10.1080/01431169308904287, 1993.

https://doi.org/10.5194/egusphere-2026-3269
Preprint. Discussion started: 19 June 2026

van Oldenborgh, G. J., Philip, S., Aalbers, E., Vautard, R., Otto, F., Haustein, K., Habets, F., Singh, R., and Cullen, H.: Rapid attribution of the May/June 2016 flood-inducing precipitation in France and Germany to climate change, Hydrology and Earth System Sciences Discussions, 2016, 1–23, https://doi.org/10.5194/hess-2016-308, 2016.

Voldoire, A.: CNRM-CERFACS CNRM-CM6-1-HR model output prepared for CMIP6 HighResMIP, https://doi.org/10.22033/ESGF/CMIP6.1387, 2019.

Voldoire, A.: CNRM-CERFACS CNRM-CM6-1 model output prepared for CMIP6 CMIP, 2023.

Volodin, E., Mortikov, E., Gritsun, A., Lykossov, V., Galin, V., Diansky, N., Gusev, A., Kostrykin, S., Iakovlev, N., Shestakova, A., and Emelina, S.: INM INM-CM5-0 model output prepared for CMIP6 CMIP abrupt-4xCO2, https://doi.org/10.22033/ESGF/CMIP6.4932, 2019.

Vrac, M.: Multivariate bias adjustment of high-dimensional climate simulations: the Rank Resampling for Distributions and Dependences (R^2D^2) bias correction, Hydrology and Earth System Sciences, 22, 3175–3196, https://doi.org/10.5194/hess-22-3175-2018, 2018.

Vrac, M. and Thao, S.: R^2D^2 v2.0: accounting for temporal dependences in multivariate bias correction via analogue rank resampling, Geoscientific Model Development, 13, 5367–5387, https://doi.org/10.5194/gmd-13-5367-2020, 2020.

Vrac, M., Drobinski, P., Merlo, A., Herrmann, M., Lavaysse, C., Li, L., and Somot, S.: Dynamical and statistical downscaling of the French Mediterranean climate: uncertainty assessment, Natural Hazards and Earth System Sciences, 12, 2769–2784, https://doi.org/10.5194/nhess-12-2769-2012, 2012.

Vrac, M., Loukos, H., Noël, T., and Defrance, D.: Should We Use Quantile-Mapping-Based Methods in a Climate Change Context? A "Perfect Model" Experiment, Climate, 13, 137, https://doi.org/10.3390/cli13070137, 2025.

Wang, Y., Zhang, J., Elmahdi, A., Jia, Y., Tang, P., Liu, P., Bao, Z., and Jin, J.: Bias correction based runoff change attribution quantification for the typical water conservation catchment in the upper yellow river basin, Theoretical and Applied Climatology, 156, 495, https://doi.org/10.1007/s00704-025-05749-9, 2025.

Wu, T., Chu, M., Dong, M., Fang, Y., Jie, W., Li, J., Li, W., Liu, Q., Shi, X., Xin, X., Yan, J., Zhang, F., Zhang, J., Zhang, L., and Zhang, Y.: BCC BCC-CSM2MR model output prepared for CMIP6 CMIP piControl, https://doi.org/10.22033/ESGF/CMIP6.3016, 2018.

Xu, K., Wang, C., and Bin, L.: Compound flood models in coastal areas: a review of methods and uncertainty analysis, Natural Hazards, 116, 469–496, https://doi.org/10.1007/s11069-022-05683-3, 2023.

Xu, K.-M.: Using the Bootstrap Method for a Statistical Significance Test of Differences between Summary Histograms, Monthly Weather Review, 134, 1442–1453, https://doi.org/10.1175/MWR3133.1, 2006.

Yang, Y., Maraun, D., Ossó, A., and Tang, J.: Increased spatial extent and likelihood of compound long-duration dry and hot events in China, 1961–2014, Natural Hazards and Earth System Sciences, 23, 693–709, https://doi.org/10.5194/nhess-23-693-2023, 2023.

Yukimoto, S., Koshiro, T., Kawai, H., Oshima, N., Yoshida, K., Urakawa, S., Tsujino, H., Deushi, M., Tanaka, T., Hosaka, M., Yoshimura, H., Shindo, E., Mizuta, R., Ishii, M., Obata, A., and Adachi, Y.: MRI MRI-ESM2.0 model output prepared for CMIP6 CMIP, https://doi.org/10.22033/ESGF/CMIP6.621, 2019.

Zscheischler, J. and Lehner, F.: Attributing Compound Events to Anthropogenic Climate Change, Bulletin of the American Meteorological Society, 103, E936–E953, https://doi.org/10.1175/BAMS-D-21-0116.1, 2022.

Zscheischler, J., Westra, S., Van Den Hurk, B. J., Seneviratne, S. I., Ward, P. J., Pitman, A., AghaKouchak, A., Bresch, D. N., Leonard, M., Wahl, T., and others: Future climate risk from compound events, Nature climate change, 8, 469–477, https://doi.org/10.1038/s41558-018-0156-3, 2018.

https://doi.org/10.5194/egusphere-2026-3269
Preprint. Discussion started: 19 June 2026

Zscheischler, J., Martius, O., Westra, S., Bevacqua, E., Raymond, C., Horton, R. M., van den Hurk, B., AghaKouchak, A., Jézéquel, A., Mahecha, M. D., and others: A typology of compound weather and climate events, Nature reviews earth & environment, 1, 333–347, https://doi.org/10.1038/s43017-020-0060-z, 2020.